Cours POWAG 2000, Summer School on Photosensitivity in Optical Waveguides And Glasses, 8-14 July 2000, Giens, France.

Kinetics of thermally activated physical processes in disordered media.

B. Poumellec

Physico-Chimie des Solides, UMR CNRS 8648, University of Paris Sud (XI), Orsay Center, 91405 Orsay, France

Content

I Problem: dynamic evolution of physical quantities in disordered media

UV written intracore Bragg gratings are now routinely used for applications in optical telecommunications or civil engineering. Most applications require a long grating lifetime. For example, in dense wavelength-division multiplexing optical communication systems, the grating-based devices should keep working to an agreed specification for 25 years in the temperature range -40°C<Θ<+80°C. Accordingly, several theoretical and(or) experimental studies dealing with accelerated lifetime tests have been carried out with a view to forecast possible degradation of the UV-induced refractive index changes [1]-[2].

For modelling the relaxation process in disordered media, several approaches can be used, an extended report can be found in the reference book of Richert and Blumen [3]. The main problem is to account for the effect of disorder on the relaxational process. This disorder can have an impact on the various steps of the physico-chemical reaction leading to relaxation of the observed quantity. For instance, if a hopping is concerned in the reaction, the disorder will appear on the hopping distance or on the waiting time, if an energy barrier is involved, the activation energy will be distributed either because the transition and/or the stable state configurations are various.

These two examples differ fundamentally on one point: the temperature will not affect in the same way the range limited or the temperature activated hopping. In particular, the dependence of the stability of refractive index with the writing or the ageing temperature [4] can be only explained by processes with distributed activation energies. Other arguments connected to structural changes in the structure reinforce this conclusion. However, a process like decoration of defect network with H will not necessary be relevant of a thermally activated process. In this paper, we consider only relaxation process involving distribution of activation energies as it is seen that this approach yield good results [1, 5] in our problems of index change.

I 1 under an external action

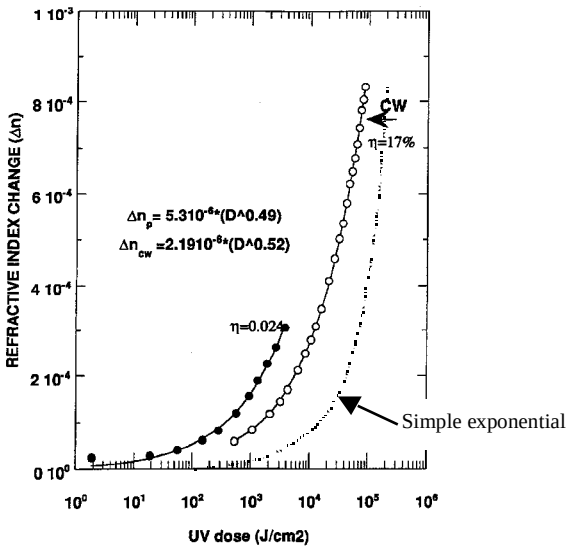

Fig. 1: Index change under UV irradiation [6].

Maybe the most important example for people working for fabricating telecommunication devices is the non exponential growth of refractive index change under UV irradiation. We can see in **fig. 1** that for pulsed 248 nm laser, the index change grows according to a power law with an exponent of 0.5 [7]. In a lot a fibers, this law is followed with an exponent between 0.25 and 0.8. We know from [8] that index change in Ge doped glasses is achieved by UV induced compaction. It is known that it is possible to achieve compaction in pure silica by the same mean [9] but it is also possible to obtain compaction by ion or electron irradiation. Primak [10] is probably the author who studied these processes the most.

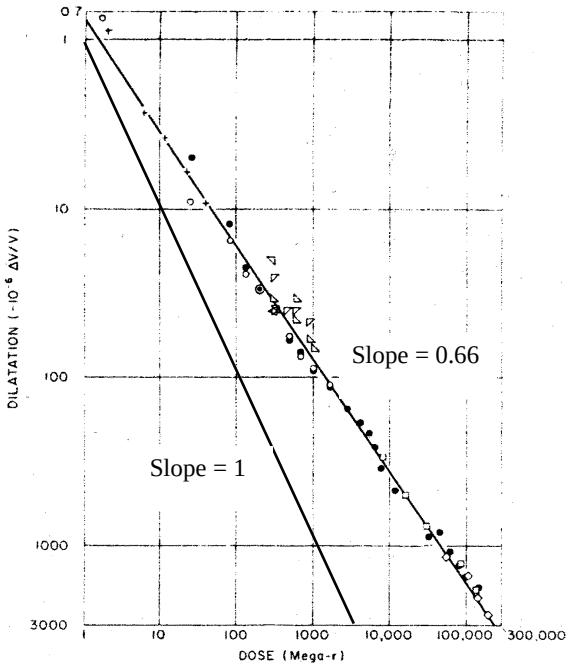

FiG. 2: electron irradiation induced compaction [10]

We can see in **fig. 2** that compaction follows a power law again with an exponent of 0.66. More recently, Allan et al. [11] shown that 193 nm irradiation in pure silica leads to densification by two-photon absorption (**fig.3**).

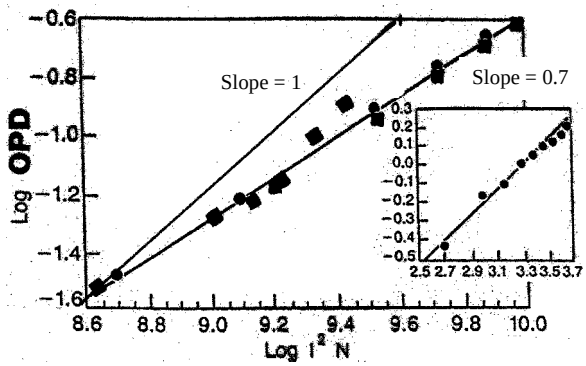

Fig. 3: Densification in fused silica under 193 nm irradiation [11]. The optical path difference follows: $OPD = a\left(I^2 N\right)^{0.7}$

We note in this case that the dose is no more the relevant parameter but I^2N where I is the power density and N the pulse number. The behaviour is a power law with an exponent of 0.7.

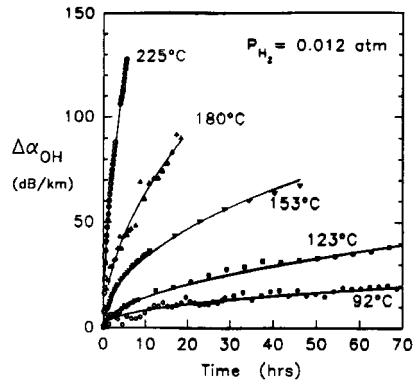

Data on OH growth measured at several temperatures for a fiber doped with Er, GeO_2, and Al_2O_3; curves are nonlinear fits to at^m.

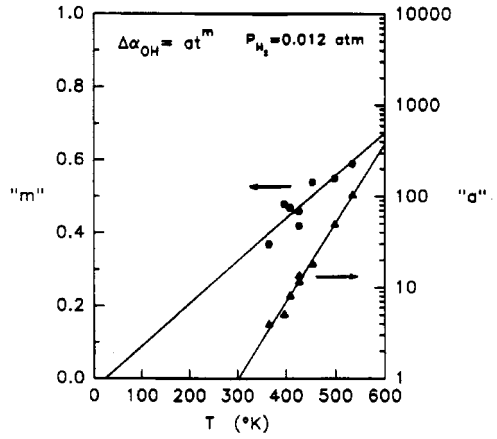

Experimentally determined values for a and *m* based on nonlinear fits to *in situ* experimental data obtained over a range of temperatures at 0.012 atm of H_2.

Fig. 4: IR darkening of the Ge doped core optical fiber [12]. The OH growth data are well described by an equation of the form: $\Delta\alpha_{OH} = a\left(t/hr\right)^m, \quad a = a_0 \exp\left(T/T_0\right)$

Another example is the IR darkening of the Ge doped core optical fibers observed under H_2 atmosphere of .012 atm (**fig. 4**). Lemaire et al [12] showed that OH vibration absorption at 1.38 μm follows a power law also in the same kind of experiment, the exponent of which increasing linearly on temperature.

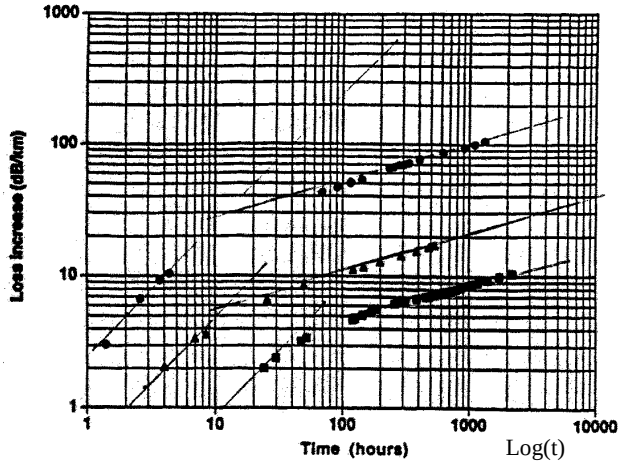

Loss increase at 1.55 µm for fiber 1 under P_H = atm for three temperatures: 150°C (circles), 80°C (triangles), and 50°C (squares).

Fig. 4: IR Hydrogen induced darkening [13].

$$\Delta\alpha_{1.55\mu m}(t) = C_{1.55} P_{H_2}^{1/2} t^{0.29} \exp\left(-\frac{6.5 kcal/mol}{RT}\right) \quad dB/km$$

Moreover they have observed that the logarithm of the pre-exponential factor evolves also linearly on temperature. The power law is not the only behaviour recorded in H_2 induced IR darkening of fibers, Rush et al. [14] shown that in the case of phosphorus doped core optical fibers, a log(t) law leads to a better fit on a larger range of time (**fig.5**).

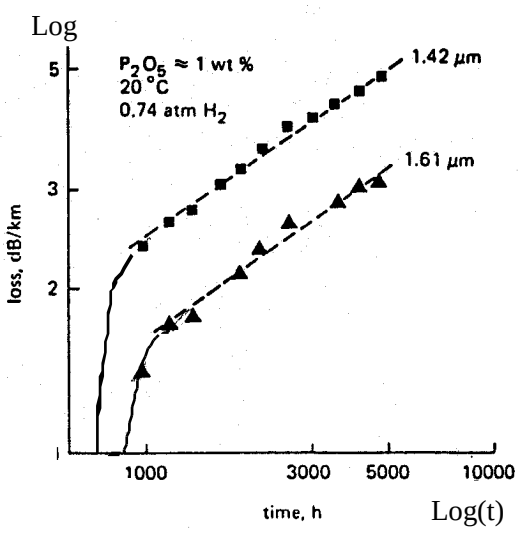

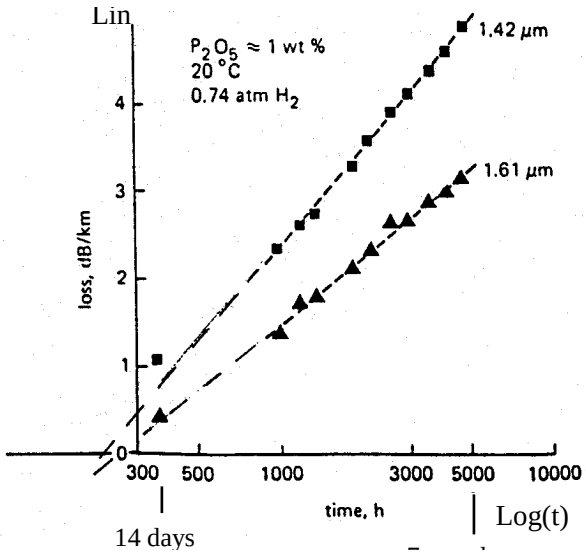

Fig. 5: IR Hydrogen induced darkening [14]

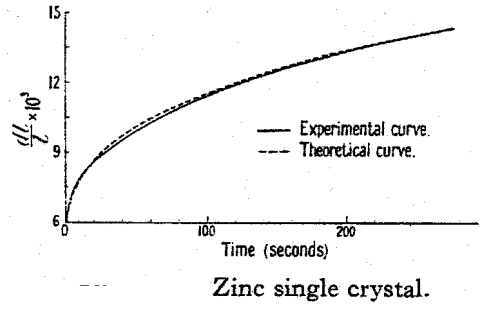

Zinc single crystal.

The same type of law has been invoked in transient creep experiments in metals. In this case, a constant distribution of sites is inferred [15] **Fig. 6**.

Fig. 6: Theory of transient creep in metals [15]

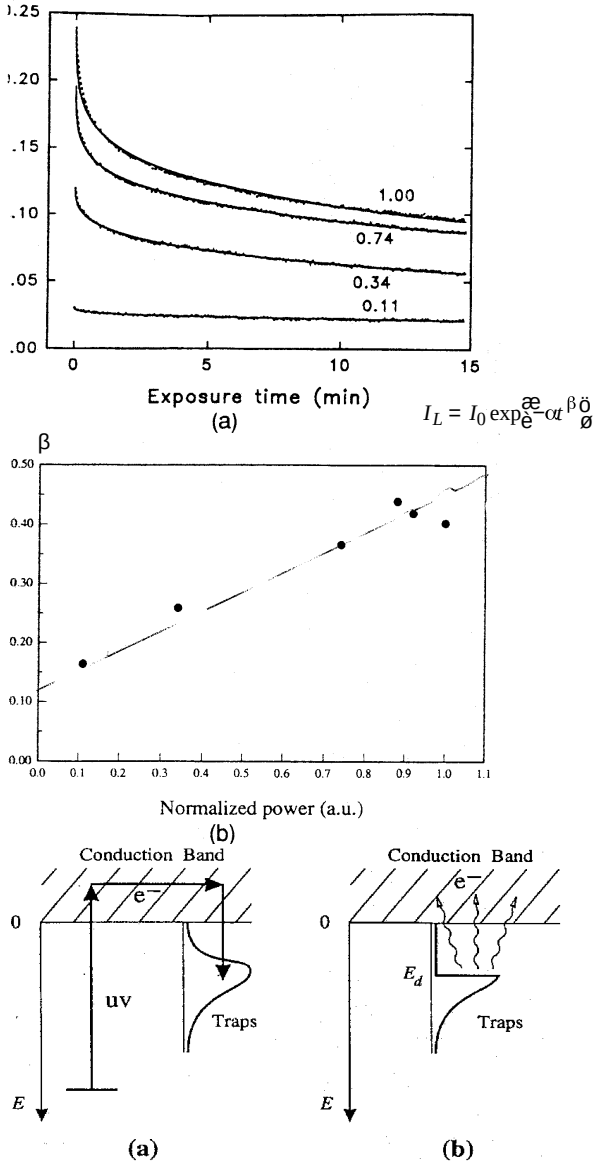

Fig. 7 : Bleaching of 400 nm luminescence by 266 nm light in Ge doped SiO_2 fibers [16].

Last example for completing the panel of non exponential behaviour of systems submitted to an external action is the bleaching of the 400 nm luminescence by 266 nm light in Ge doped core optical fibers (**Fig.7**). In that case, a stretched exponential law is used ($\exp(-at^{\alpha})$) and the exponent α is found depending linearly on power density [16]. Of course, this list is not exhaustive and is just made to show the spreading of the non exponential behaviour.

It is valuable to see that non exponential processes occur also spontaneously without any external action.

I 2 thermal relaxation

Of course, the most well known example in our field is the UV induced refractive index change relaxation (**fig. 8**). The most popular law in this field is the inverse power law or sigmoidal law studied by Erdogan et al. [17, 18]: $1/(1+at^{\alpha})$ (fig. 43 e). It is based on a energy distribution of trapping sites according to a bell shape curve with a suitable analytical form. In that case, authors showed that exponent α is linearly dependent on temperature (as in the case of H_2 induced IR darkening).

Fig. 8: Erdogan model . [17, 18]. a: uniform population whatever the trapping energy. b: progressive trap depopulation according to the tapping energy.

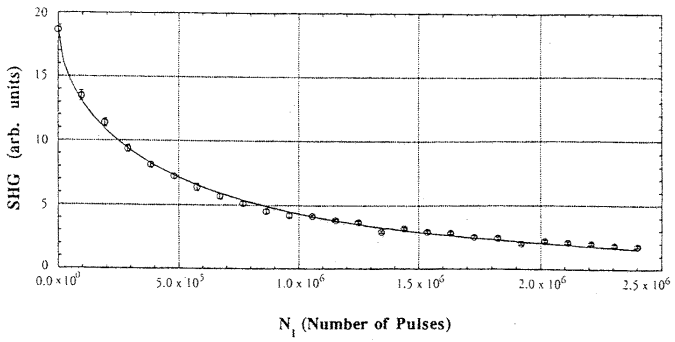

Close to UV induced refractive change, the encoded SHG by irradiation with fundamental 1.064 μm and second harmonic 532 nm is found to decrease following a stretched exponential law (**fig. 9** [19]).

Fig. 9: Relaxation of second harmonic generation [19]

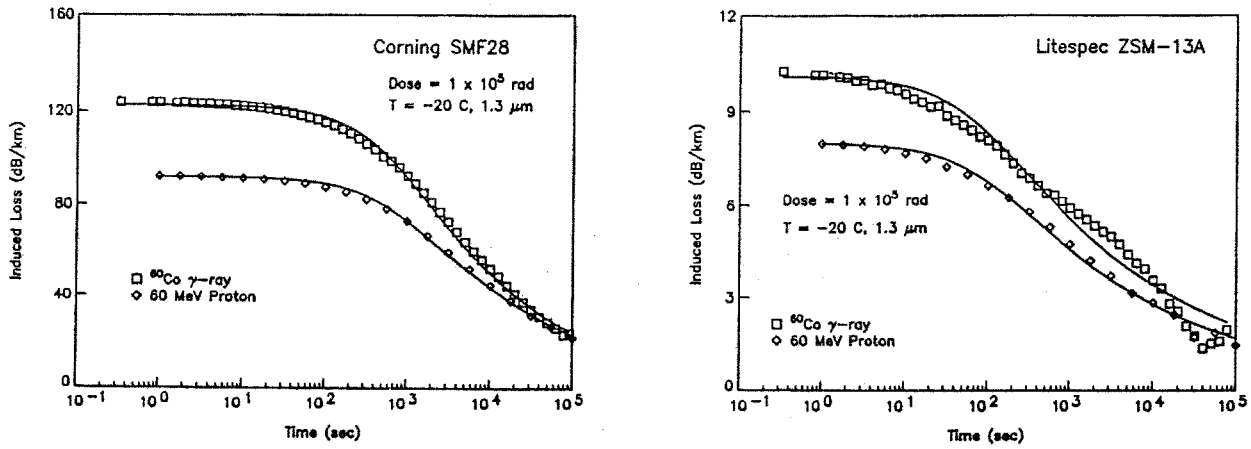

Recovery of the loss induced in (a) Corning SMF-28 and (b) Litespec ZSM single mode fibers by an ionizing dose of 10^5 rad(Si) from either a ^{60}Co γ-ray source or protons from a cyclotron.

Fig. 10: Recovery of gamma induced losses in fibers [20].

Irradiation with more energetic photon (gamma) induces optical losses following a power law in classical SMF28 Corning fiber [20]. This photodarkening relaxes following a n order kinetics according to the authors which has no physical basis but plays the role of non exponential kinetics (**fig. 10**).

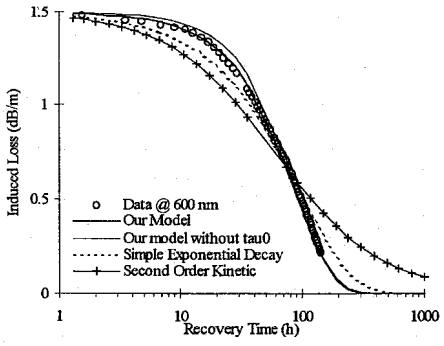

Comparison of recovery models in the case of fibre A1 during the 2nd recovery (for all models q_0=1.5 dB/m, for our model, see eq.(2), τ=104.5 h and τ_σ=358.4 h).

Fig. 11: NbOHC band recovery after gamma irradiation [22].

A part of the optical losses induced by gamma irradiation is the production of non bonding oxygen hole centers i.e. a pending bond on non bridging oxygen. Deparis et al. [22] showed that a good fit is obtained of the recovery using a peculiar stretched exponential function (**fig. 11**):

$$Loss = Loss_0 \exp\left(-\frac{t}{\tau_0} - \left(\frac{t}{\tau}\right)^{3/2}\right)$$

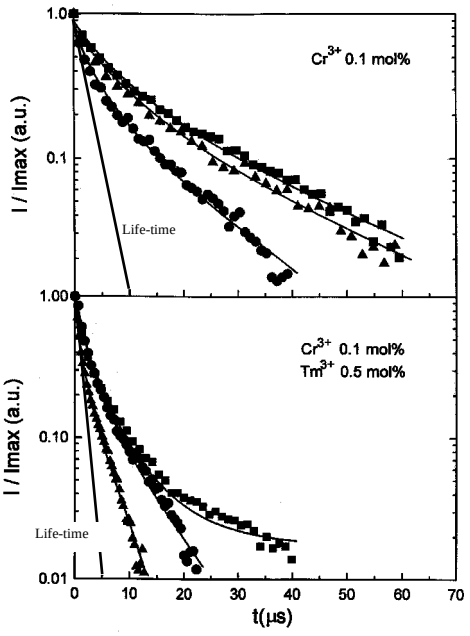

Fig. 12 $^4T_2 \rightarrow {}^4A_2$ emission from Cr^{3+} (735 nm) [21].

Same kind of recovery is the luminescence collected after, for instance, Cr^{3+} excitation in alkaline disilicate glasses. The number of photons collected is the result of relaxation of excited sites having various lifetime due to various

environment of the Cr ion. Therefore, short lifetimes are seen at the beginning and long ones at the end (**fig. 12** [21]).

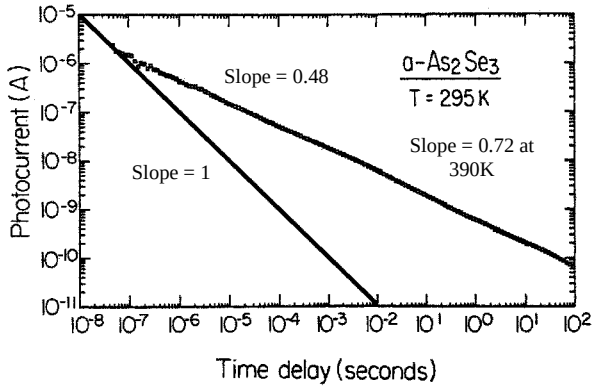

Photocurrent at room temperature in glassy As_2Se_3, resulting from a 10-ns-long pulse of light at $t = 0$.

Fig. 13: Band tail photocurrent in As_2Se_3 glass. $i = at^{\alpha}$, the exponent varies on T like $-1+T/T_0$. A Poisson distribution of trapping sites is deduced.

This excitation is of the same nature than electron excitation followed by trapping (**fig. 13**). Don Monroe [23] showed that the non exponential behaviour of the electric current due to relaxation of trapped electron after 1.6 eV excitation in As_2Se_3, is due to a distribution of trapping sites according to a Poisson distribution and corresponding to a band tail trapping.

Fig. 14: Viscosity below glass transition temperature [24]: $\eta_{apparent} = \frac{1-\psi}{3d\psi/dt}$ *with* $1-\psi = \exp\left[-(t/\tau)^{b}\right]$

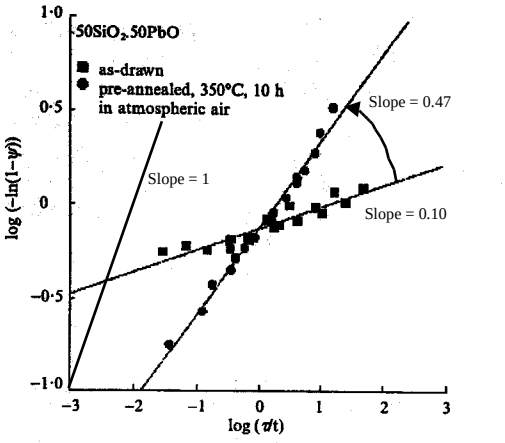

Plot of log(t/τ) versus log(−ln(1−ψ)) for SP55 glass

Non exponential relaxation occurs not only after irradiation. **Fig. 14** from Kroide et al [24] is just an example that viscosity below glass transition temperature (i.e. relaxation of glass after a stress perturbation) is also of the same nature. Stretched exponential behaviour is found with exponent smaller than one, as usual. The exponent seems to depend on the fictive temperature. This is relevant of change of atomic configurations in glasses from site to site toward a more stable arrangement.

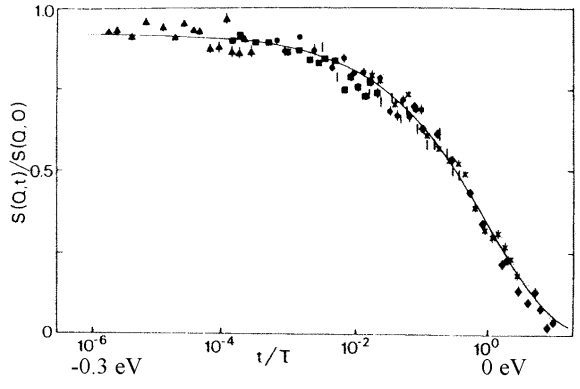

Scaling representation of the neutron spin-echo data for relaxation of cis–trans polybutadiene at the maximum $Q = Q_1$ of the structure factor, $S(Q)$, where t is rescaled by τ so that the filled triangle data for $T = 200$ K lie to the left, while the diamond data for 280 K lie to the right. The smooth line is the Kohlrausch fit with $\beta = 0.45(2)$, all reproduced from Ref. [7] for the reader's convenience. Note that the fit spans more than six decades in the abcissa.

Fig. 15: cis-trans isomerisation in polybutadiene [25]

Similar processes occur in polybutadiene due to cis-trans isomerisation (**fig. 15** [25]). Finally, the last example shows that viscosity relaxation leads to stress relaxation especially in optical fiber after drawing. Mohanna et al. [26] found that stress decrease obeys to a stretched exponential with an exponent increasing linearly on temperature **(fig.16)** as it was for H_2 induced IR darkening (fig.4).

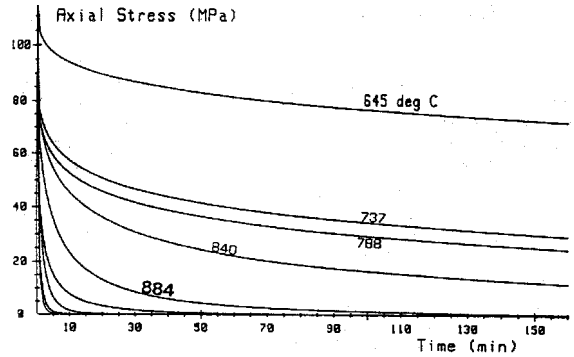

Stress release curves for temperatures of Table I.

TABLE I
THE a AND b DATA AT DIFFERENT TEMPERATURES ($\sigma = \sigma_0 \exp -(at)^b$)

T(°C)	1080	1028	979	932	883	840	788	737	645
"a"	2.89	2.39	1.12	1.06	0.28	.079	.036	.022	.0005
"b"	0.68	0.63	0.61	0.42	0.45	0.32	0.24	0.24	0.3

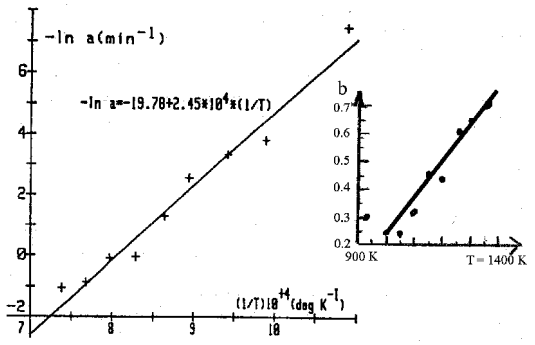

Variation of a and b parameters on temperature

TABLE II
INTERNAL STRESS RELAXATION AFTER 24 YEARS AT DIFFERENT TEMPERATURES (σ_0 = 115 MPa)

T (°C)	3	10	25	125
σ(25 years)	114.9998	114.9996	114.9988	114.798
(1-σ/σ0) %	1.9*10-4	3.3*10-3	1.0*10-3	0.175

Fig. 16 Stress relaxation in Ge doped fibers [26]. The equation is $\sigma = \sigma_0 \exp\left[-(at)^b\right]$

In the following section, we describe the approach in the frame of distributed activation energy case, which can be used to model the various experimental behaviour shown above. This theory applied if the distribution function does not change along the reaction i.e. if the medium or long range order of the glass structure is not modified during the reaction. In other words, if the reaction is local. If not, extension of the theory can be developed but is out the scope at the present time.

II Modelling

The methods now widely used and introduced in our field by Lemaire et al. in 1984 [27] for hydrogen induced darkening and Erdogan et al. in 1994 [1, 17] for Bragg grating stability is based on numerous previous works. The history begins with Kohlrausch in 1847 [28] studying the electric discharge of a Leyde bottle. He found a stretched exponential behaviour with an exponent of 0.43. Latter in 1876, Hopkinson proposed another relaxation function for dielectric: Bt^{-n}. In 1893 Wiechert suggested that relaxation energy in solids are distributed according to a gaussian. In 1907, Von Schweidler introduced the concept of relaxation time. In 1913, Wagner suggested that relaxation time was governed by a probability function which was a gaussian actually. At this date, everything is available for allowing Vand [29] to propose two experimental methods for studying the activation energy barrier distribution: the isothermal and tempering annealing. He defined from a first order kinetics a cutting energy, showed that the distribution function is the derivative of the physical quantity according to this energy, studied the error introduced by this approximation. This is really an important step for the study of disordered media. Then, in 1955, Primak [30] applied the Vand approach to kinetics order larger than one but he notes that one order kinetics is the most likely in solids. In 1960, Primak [31] goes on in studying the isochronous method. He made a lot of experiments in silica especially about radiation induced compaction or dilatation. He improved a little bit the Vand method. After that date, several publications dealing with distributed kinetics appear but without mentioning the origin. Tiedje and Orenstein (1980) [32] invoked a demarcation energy which is the Vand cutting energy. In 1986, Don Monroe et al. [23] use the previous work for interpretation of the photocurrent decay in selenium arsenide. In 1991, Miller [33] developed a predictive formalism to describe generalised activated physical processes. In 1992, Lemaire [34], in 1994 Erdogan [1, 17], applied to optical fibers. In 1996 Van den Brink [35] defined a master curve in viscoelastic relaxation in using several Maxwell elements (simple exponentials). In 1997 Kannan et al. [36], use this master curve concept for predictive ends in optical fibers.

We are now describing the theory of distributed kinetics allowing to analyse experimental results but before that, let us understand the difference between a non-distributed kinetics (simple reaction pathways - SIREPA) and a distributed one (variable reaction pathways - VAREPA).

II.1 exponential versus non exponential kinetics (introduction to theory)

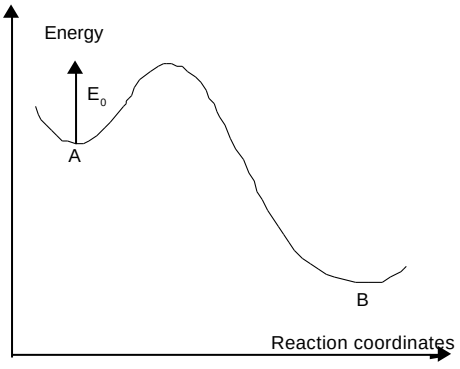

Fig. 17 Chemical pathway between A and B.

An exponential kinetics is the time behaviour of a first order reaction. We can write:

$A \xrightarrow{k} B, \quad E_0, \quad k = k_0 \exp\left(-\frac{E_0}{k_B T}\right)$ where E_0 is the unique activation energy of the reaction i.e. the energy barrier to transform A in B in fig.17. The rate equation for this reaction is $\frac{dA}{dt} = -kA, \quad A + B = A_0$. The computation of the A or B contents leads to the following expressions: $\begin{aligned} A &= A_0 \exp(-kt) \\ B &= A_0\left[1 - \exp(-kt)\right] \end{aligned}$. We can notice that if we plot the quantity

B versus time (fig. 18a), the curve will exhibit a linear behaviour at the origin before saturation. If we plot $\log(A_0/(A_0-B))$ against time (fig; 18b), we will get a linear behaviour until the infinity.

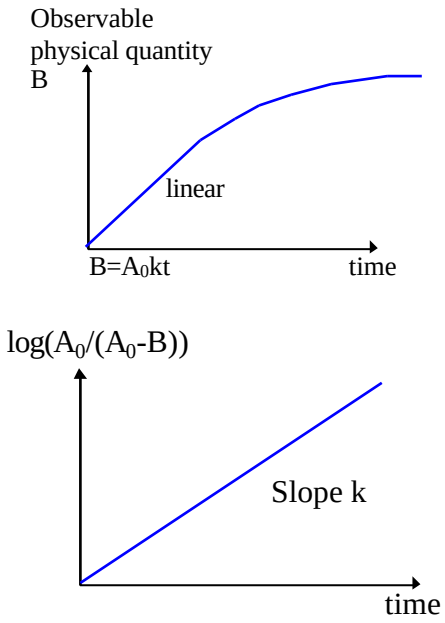

Fig. 18: SIREPA. a: B versus time. b: $\log(A_0/(A_0-B))$ versus time.

A non-exponential behaviour like $at^{\alpha}/(1+ at^{\alpha})$ is quite different. If we plot B versus time (fig. 19a), the curve exhibits an infinite slope at the origin, then the slope decreases strongly and finally the evolution is slower than for an exponential behaviour. Translated in term of exponential equation, we can see that the rate constant k decreases on time, there is a strengthening. If we plot $\log(A_0/(A_0-B))$ versus time in fig. 19b, the plot is not at all linear but exhibits an infinite slope at the origin and then the slope decreases strongly.

Another plot usually performed in this case is a log-log plot (fig. 20). In this frame, the exponential equation will exhibit a slope of unity at the origin whereas the power law will have a slope α usually smaller than 1.

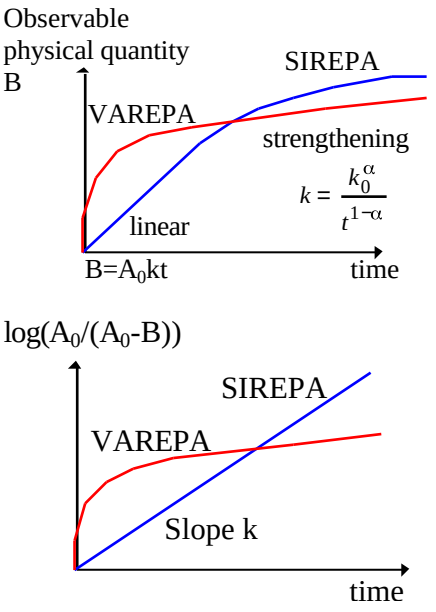

Fig. 19: a: B versus time. b: $\log(A_0/(A_0-B))$ versus time.

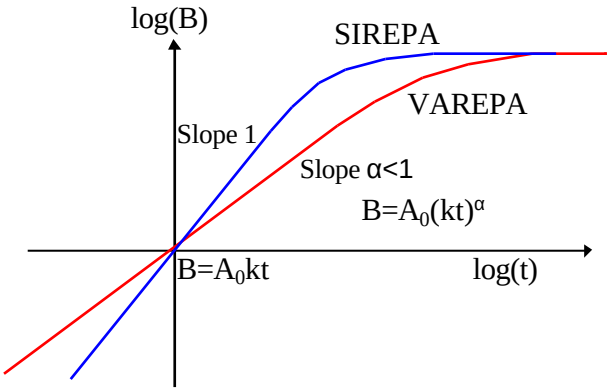

Fig. 20: VAREPA kinetics compared SIREPA. lob(B) versus log(time).

More subtle is the thermal behaviour of these two kinds of kinetics. The reverse reaction (if any) will work through energy barriers complementary to the formation energy difference between A and B species (see section IV.1). The two kinetics can be differentiated sometimes by their thermal relaxation. In an isochronous plot (B/B_0 versus T) fig. 21, the exponential behaviour will give rise to the same sigmoidal plot whatever the temperature or the duration of the writing (reaction $A \rightarrow B$). For a non-exponential behaviour, the stability increases on writing temperature until a limit and on duration of writing. It is just like a nail more and more driven into a wooden piece, the stability is improved.

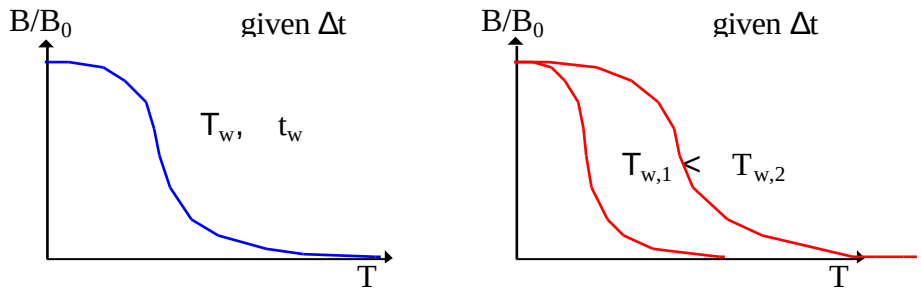

Fig. 21: Isochronous curves. a: SIREPA. b: VAREPA.

II.2 kinetics of writing

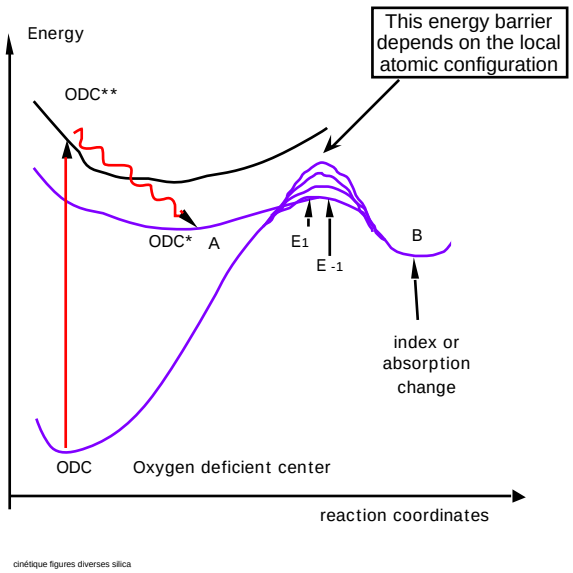

Fig. 22: example of physical chemical reaction, an absorption step followed by a thermally activated reaction.

We are now going to model the kinetics of writing. This is based on several assumptions.

A) First group of assumptions

1) we imagine easily that the reaction leading to refractive index change contains an absorption step on a species (for instance Oxygen Deficient Center) following sometimes by a relaxation to another excited level in fig. 22. Then, several pathways are possible (one to luminescence, another one to bond breaking, migration, structural rearrangement). All of them contribute finally to refractive index change. The first assumption we make here is that only one elementary reaction is concerned: the limiting reaction of the process. We can write the reaction A→B.

2) the second assumption is that it is thermally activated (with an energy E)

3) the third assumption is that activation energy is distributed. This means that chemical pathways are variable depending on the configuration distribution of the transition state and/or the initial stable states throughout the glass. This is the origin of ergodicity lost because space-time points are no more equivalent. The reaction is faster in some places than elsewhere. This is also an heterogeneity but not at a macroscopic level just at a microscopic one.

We can call the relevant distribution g(E) and chosen it normalised. If g is relevant of a thermal disorder, a gaussian distribution seems likely, if g is relevant of a diffusionnal process a Poisson distribution is better but also other approximation has been used: differentiation of a sigmoid [1, 17], top hat function [5]. We will see also that g(E) can be obtained from the experiment and then approximated if necessary. At this step of the description, calling x the advancement of the reaction, depending on the activation energy E and the time, we have:

$$[B]_T(t) = A_0 \int_0^{\infty} x(E,t,T)g(E)dE \qquad (1)$$

These assumptions constitute the first group of assumptions which are mainly connected to disorder.

B) The assumption on the reaction (connection with time and temperature).

This assumption will allow to compute the time dependence properly.

Most of the elementary reaction are first order, some are second order when two species associate but these are less likely. So, it is not so severe to assume that A→B is a first order reaction with a rate constant $k(E,T)=k_0\exp(-E/k_BT)$ (second order reaction is investigated in section V1). This allows to compute the advancement degree $x(E,t,T)=1-\exp(-k(E,T).t)$. Usually, the B integral is not computable analytically and thus extraction of g(E) is very difficult. A simplification of the integral is required to handle complex cases. Here, we can observe that $x(E)_t$ is a very steep function of E in such a way that below a demarcation energy (E_d) x is equal to 1 and above it is equal to 0 (fig. 23). This clever remark made by Vand [29] leads to simplify the equation usefully.

$$[B]_T(t) = A_0 \int_0^{E_d(t,T)} g(E)\,dE \qquad (2)$$

To properly define E_d, we can chose the value where $x(E)_{t,T}$ varies the most (the steepest variation defined by $\frac{\partial^2 x}{\partial E^2} = 0$, in this case, we get $E_d=k_BT.\ln(k_0t)$.

Rem. 1: it is worth noticing that the reaction properties appears now only in $E_d(t,T)$ on one hand (the bound of the integral) and the structural disorder appears in the integrand on the other hand.

Rem 2: the demarcation energy approximation is valid if g(E) varies slower than x(E,t,T).

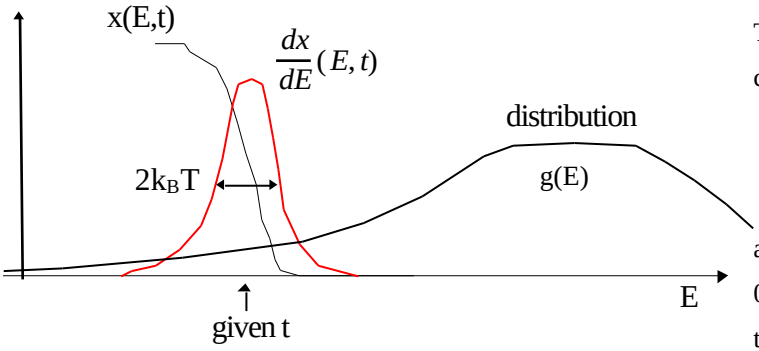

Fig. 23: comparison of widths between x(E,t) and g(E).

The width of dx/dE is 2kT. Otherwise, a correction has to be added to the integral [33]:

$$-k_BT\sum_{k=0}^{k=\infty} c_{k+1}\left.\frac{d^k g(E)}{d(E/k_BT)^k}\right|_{e=e_d}$$ where c_{k+1} are constant close to unity (c_1=Euler constant 0.577, c_2= .989, c_3=.907, c_4= .981, c_5 also and then equal to 0.999).

Rem. 3: $\frac{dB}{dE_d} = A_0 g(E_d)$. The differentiation of B against E_d yields the shape of distribution function.

Rem. 4: $E_d=k_BT\ln(k_0t)$ => $B(E_d)$ exhibits same shape than B(T for given t) or B(ln(t) for given T)

If g(E) does not depend on T, isochrons and isotherms are equivalents

For isotherms Δn should be measured at the same temperature.

For isochronous annealing, there is a criterion on the temperature step and duration of the step (see section IV2).

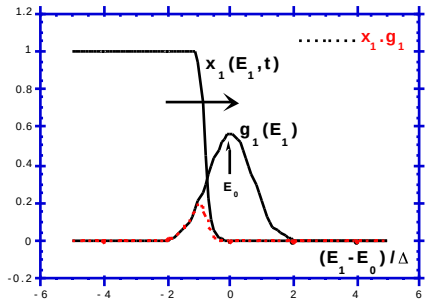

Fig. 24: progress of advancement degree along the distribution function.

For a given time, $[B](t)$ is the area under the dotted curve in the figure 24. As t increases, x_1 moves to the right hand side and more difficult pathways are used.

C) Examples for time dependence computation

The integration using a gaussian distribution...

$g_1(E) = \frac{1}{\Delta\sqrt{\pi}} \exp\left(-\left(\frac{E - E_0}{\Delta}\right)^2\right)$ with $E_0 \tilde{>} 2\Delta$ centered on E_0; width Δ

...yields:

$$[B](t) = A_0 \frac{1}{\Delta\sqrt{\pi}} \int_0^{E_d(t)} \exp\left(-\left(\frac{E - E_0}{\Delta}\right)^2\right) dE_1$$

$$[B](t) = \frac{A_0}{2}\left[1 + f_{err}\left(\frac{E_d - E_0}{\Delta}\right)\right]$$ where f_{err} is the error function.

Sigmoid differentiation distribution

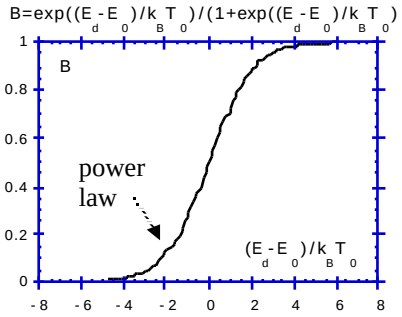

$$g_1(E) = \frac{1}{k_B T_0} \frac{\exp\left(\frac{E_1 - E_0}{k_B T_0}\right)}{\left[1+\exp\left(\frac{E_1 - E_0}{k_B T_0}\right)\right]^2}$$

$$[B](t) = A_0 \int_0^{E_d(t)} g_1(E_1)dE_1 \approx A_0 \frac{\exp\left(\frac{E_d - E_0}{k_B T_0}\right)}{1+\exp\left(\frac{E_d - E_0}{k_B T_0}\right)} = A_0 \frac{\left(k_1^0 t\right)^{T/T_0} \exp\left(\frac{-E_0}{k_B T_0}\right)}{1+\left(k_1^0 t\right)^{T/T_0} \exp\left(\frac{-E_0}{k_B T_0}\right)}$$

Poisson distribution

$$g_1(E) = \frac{1}{k_B T_0} \exp\left(\frac{-E_1}{k_B T_0}\right)$$

$$[B](t) = A_0 \int_0^{E_d(t)} g_1(E_1)dE_1 = A_0\left[1 - \exp\left(\frac{-E_1}{k_B T_0}\right)\right] = A_0\left[1 - \left(k_1^0 t\right)^{-T/T_0}\right]$$

condition on t: $t > 1/k_1^0$

D) How to obtain k_0 and g(E) (fig.25)

1) Measurement of several isochrons or isotherms

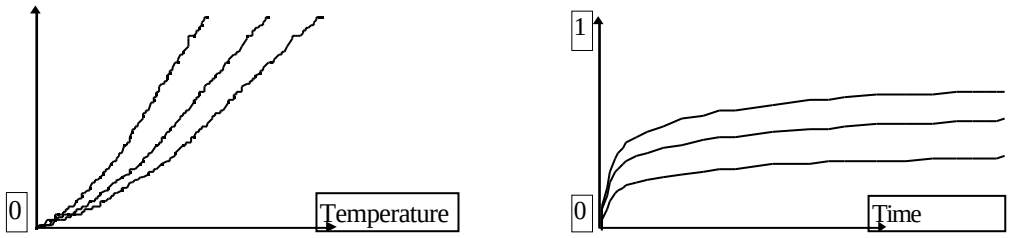

Replotting against a new abscise

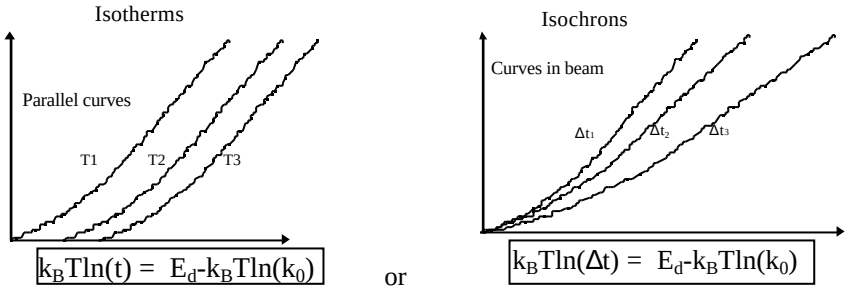

2) k_0 fitting for curves collapsing

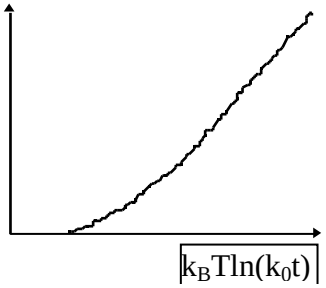

3) differentiation

$$\frac{d[B](t)}{dE_d}\Big|_t = A_0 g_1(E_d(t))$$

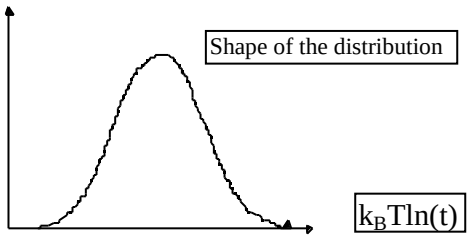

N.B. k_0 - g(E) separation

II.3 relaxation

The hypotheses for modelling the relaxation behaviour ($A \leftarrow B$) are basically the same as for the forward reaction ($A \rightarrow B$). There is a symmetry in the approach. The only difference is that the starting population is different. Whereas all sites are under A form for forward reaction, it may be under A or B form for relaxation i.e. the writing has not transformed all A content but only the easiest part (non saturated writing). When the writing kinetics was completed or the writing kinetics is not distributed, the same computation as in II 2 applies in replacing A by B and vice-versa, and considering that the activation energy is for the backward reaction and also that the distribution is different (see below).

Otherwise, it is necessary to consider a starting distribution for B which is equal to $A_0 x_+(E_+, t_w, T_w) g_+(E_+)$. i.e. the advancement degree times the distribution function. We have to consider the following expression for B content and at time t at temperature T when forward pathways are independent on backward pathways.

$$B(t,T) = A_0 \int_0^\infty \int_0^\infty x_+(E_+,t_w,T_w)\left[1 - x_-(E_-,t,T)\right] g_+(E_+) g_-(E_-)\, dE_+ dE_-$$

This is equivalent to:

$$B(t,T) = \underbrace{A_0 \int_0^\infty x_+(E_+,t_w,T_w) g_+(E_+)\, dE}_{B_0(t_w,T_w)} \int_0^\infty \left[1 - x_-(E_-,t,T)\right] g_-(E_-)\, dE_-$$

Therefore, the same approach as in II2 can be used again for solving this integral. Otherwise, the energy of the reverse reaction can be related to energy of the forward reaction and $B_0(E_+)$ become $B'_0(E_-)$. Let us recall now the way of computations which are applicable to all cases.

A) First group of assumptions

1) one elementary reaction $A \xleftrightarrow{k} B$ (limiting process), A → B is the writing process

2) thermal activation, E_-, $k(E_-)=k_0.\exp(-E_-/k_BT)$

3) E_- is distributed

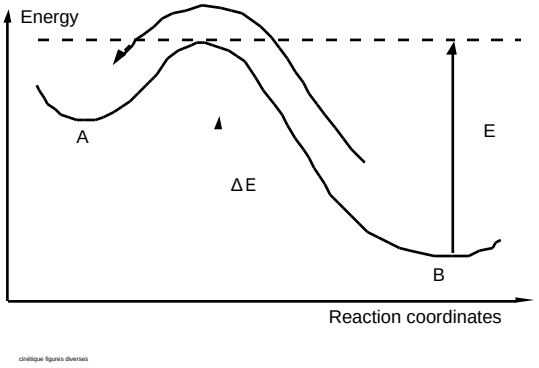

Fig. 26: reaction pathway for reverse reaction.

- variable chemical pathways
- the saddle point or the B state are sensitive to various structural configurations
- g(E) is the distribution function for backward reaction, it can be gaussian for a thermal disorder or Poisson for a diffusionnal disorder or differentiation of a sigmoid or also top hat function

$$[B]_T(t) = \int_0^\infty B_0(E_-)\left(1 - x_-(E_-,t)\right) g_-(E_-)\, dE_-$$

$B_0(E)$ initial distribution of sites according eventually to the activation energy. 1-x is the degree of retardation.

B) Second group of assumptions

(towards the computation of time dependence)

1) first order reaction (most of solid state reactions)

$$A \xleftrightarrow{k} B \qquad \frac{dx_-}{dt} = k_-\left(1 - x_-\right) \quad x_-(E_-,t,T) = 1 - \exp(-k_-(E_-,T)t)$$

2) demarcation energy, E_d

$$x_-(E_-,t,T) \begin{cases} = 1 & \text{for low energies (reaction completed)} \\ = 0 & \text{for high energies (reaction not begun)} \end{cases}$$

=> when $x_-(E_-,t,T)$ varies faster than $g_-(E_-)$, it can be approximated to an Heaviside function at energy E_d^-

$$[B]_T(t) = \int_0^\infty B_0(E_-)\exp\left(-k_-(E,T)t\right) g_-(E_-)\, dE_- = \int_{E_d^-}^\infty B_0(E_-) g_-(E_-)\, dE_-$$

- E_d is properly defined by $\left.\frac{\partial^2 x_-}{\partial E^2}\right|_{E=E_d} = 0$ => $E_d = k_B T \ln(k_0 t)$ the reaction properties are localised in E_d , (the disorder appears in g(E)). Finally B(t,T) is the area under the dotted curve in the figure27. The retardation degree (1—x) in progressing erases the B distribution.

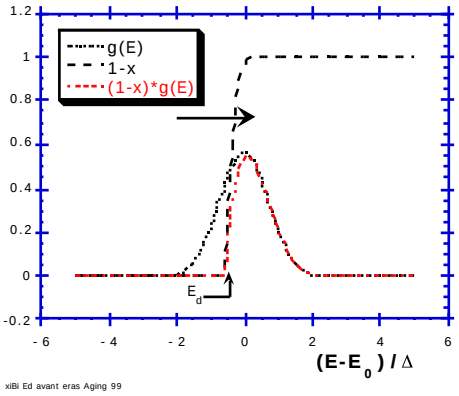

Fig. 27: reaction progresses by removing B sites, from less stables to the most stables sites

Consequences of the theory

- stability increases along the time: hardening

C) A few examples of time dependence computations assuming $B_0(E)=B_0$

If g(E) is gaussian then

$$[B](t,T) = B_0\left(\frac{1 - f_{err}\left(\frac{k_B T \ln(k_0 t) - E_0}{\Delta}\right)}{2}\right) \approx \underbrace{B_0\left(1 - a(k_0 t)^{\frac{k_B T}{\Delta}}\right)}_{\text{for low t}}$$

If g(E) is a Poisson distribution then $[B](t,T) = a(k_0 t)^{-\frac{k_B T}{\Delta}}$ Δ is the width of the distribution.

If g(E) is a differentiation of a sigmoid then $[B](t,T) = B_0\left(\frac{1}{1 + a(k_0 t)^{\frac{3k_B T}{\Delta}}}\right)$

If g(E) is a top-hat of width Δ then $[B](t,T) = B_0\left(\frac{E_{\max} - k_B T \ln(k_0 t)}{\Delta}\right)$

etc...

D) Incomplete forward reaction in the case of dependent backward and forward pathways ($B_0(E)$) [37]

If there is a dependence between the writing and the relaxation, it is valuable to know the relation between E_+ and E_-. We can solve the problem rather easily when the forward and backward reaction use the same pathways. In this case, $E_- - E_+ = \Delta E$ where ΔE is the formation energy difference between A and B (fig. 28).

We consider the initial distribution of B, $B_0(E_+, t_w, T_w) = A_0\left[1 - \exp\left(-k(E_+, T_w) t_w\right)\right]$ in the following integral

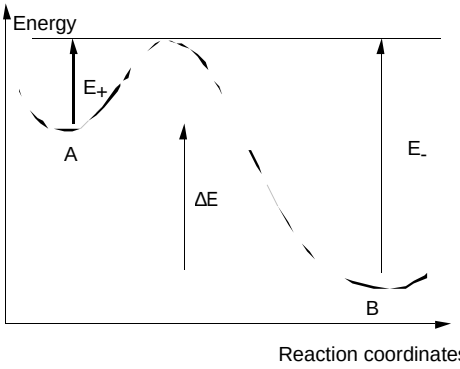

Fig. 28: relation between activation energies

$$B(t,T)=\int_0^{\infty} B_0\left(E_+,t_w,T_w\right)\exp\left(-k_-(E_-,T)\right)g(E_-)\,dE$$

Hyp: the forward and backward pathways are the same => $E_- - E_+ = \Delta E$

$$A \leftrightarrow B \quad k_{-1}=k_{-1}^0\exp\left(-\frac{E_{-1}}{k_BT}\right)$$

For each E_{-1}, $x_{-1}\left(E_{-1},t\right)=1-\exp\left(-k_{-1}\left(E_{-1}\right)t\right)$

$$B(t,T)=A_0\int_0^{\infty}\underbrace{\left[1-\exp\left(-k_+(E_+,T_w)t_w\right)\right]}_{define\,E_d^{+'}}\underbrace{\exp\left(-k_-(E_-,T)\right)}_{define\,E_d^{-}}g(E_-)dE_-$$

in the scale of E_-, we define $E_d^{+'}=E_d^{+}+\Delta E$ considering that each E_+ is related to a E_- which is $E_++\Delta E$. This means that the function $1-\exp(-k_+t)$ commuting at E^+_d in the E_+ scale commutes at $E_d^{+}+\Delta E$ in the scale of E i.e. there is no more B above this value or there is no reverse reaction above $E^+_d+\Delta E$ (fig. 29), so

$$B(t,T)=A_0\int_{E_d^-}^{E_d^++\Delta E} g(E_-)dE_- = A_0\int_{E_d^--\Delta E}^{E_d^+} g(E_+)dE_+$$

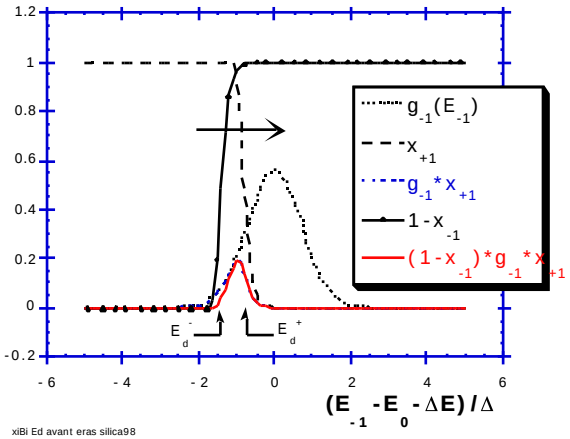

Fig. 29: erasure of incomplete distribution.

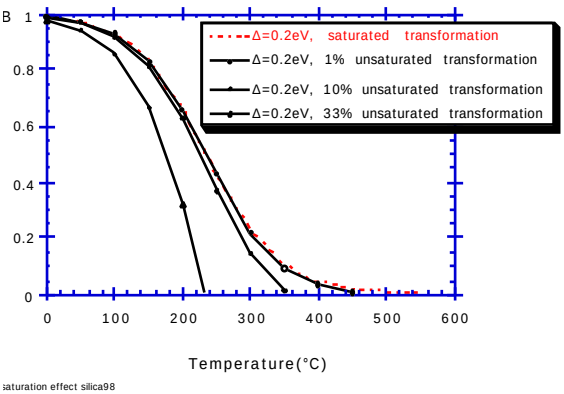

Fig. 30: the unsaturated writing leads in this case to disymmetrical isochronal curves.

D1) Gaussian distribution

$$g_1(E)=\frac{1}{\Delta\sqrt{\pi}}\exp\left(-\left(\frac{E-E_0}{\Delta}\right)^2\right) \quad \text{with} \quad E_0 \gtrsim 2\Delta$$

$$[B](t,T)=A_0\int_{E_d^--\Delta E=k_BT\ln\left(k_{-1}^0t\right)-\Delta E}^{E_d^+=k_BT_w\ln\left(k_1^0t_w\right)} g_1\left(E_1\right)dE_1$$

$$=A_0\left[1+f_{err}\left(\frac{E_1-E_0}{\Delta}\right)\right]_{k_BT\ln\left(k_{-1}^0t\right)-\Delta E}^{k_BT_w\ln\left(k_1^0t_w\right)}$$

defining $\eta\left(t_w,T_w\right)$ the proportion to saturation by

$$\eta=\frac{1+f_{err}\left(\frac{k_BT_w\ln\left(k_1^0t_w\right)-E_0}{\Delta}\right)}{2} \quad and \quad B_0=A_0\eta$$

$$we\ \ get\ \ [B](t,T)=B_0\frac{2\eta-1-f_{err}\left(\frac{k_BT\ln\left(k_{-1}^0t\right)-\Delta E-E_0}{\Delta}\right)}{2\eta}$$

Isochrons B(T) curves are plotted for several values of η in fig. 30.

We find that as η increases on t_w and T_w

$\frac{2\eta-1}{2\eta}$ and $\frac{[B]}{B_0}$ increases, thus the stability increases. This arises from the fact that high activation energy pathways are used or more stable sites are produced. This will have a real importance on the bandwidth stability of Bragg gratings in a few cases (see section VI).

After annealing

The easiest pathways are removed. The most difficult ones remain = the stability is increased.

D2) Sigmoid differentiation distribution

$$g_1(E_1)=\frac{1}{k_BT_0}\frac{\exp\left(\frac{E_1-E_0}{k_BT_0}\right)}{\left[1+\exp\left(\frac{E_1-E_0}{k_BT_0}\right)\right]^2}$$

When the forward reaction is completed, the erasure follows the equation below:

$$[B](t)=\frac{A_0}{1+\left(k_{-1}^0 t\right)^{\frac{T}{T_0}}\exp\left(\frac{-\Delta E-E_0}{k_BT_0}\right)}$$

however, when it is not, t_w and T_w appear in the equation.

$$\frac{[B](t)}{B_0}=\frac{1-\frac{\left(k_{-1}^0 t\right)^{\frac{T}{T_0}}\exp\left(\frac{-\Delta E}{k_BT_0}\right)}{\left(k_1^0 t_w\right)^{\frac{T_w}{T_0}}}}{1+\left(k_{-1}^0 t\right)^{\frac{T}{T_0}}\exp\left(\frac{-\Delta E-E_0}{k_BT_0}\right)}$$

Defining $\eta=\frac{1}{1+\left(k_1^0 t_w\right)^{\frac{T_w}{T_0}}}$ the proportion to saturation, we get

$$\frac{[B](t)}{B_1}=\frac{1-\left(k_{-1}^0 t\right)^{\frac{T}{T_0}}\exp\left(-\frac{E_0+\Delta E}{k_BT_0}\right)(1-\eta)}{1+\left(k_{-1}^0 t\right)^{\frac{T}{T_0}}\exp\left(-\frac{E_0+\Delta E}{k_BT_0}\right)}$$

D3) Poisson distribution

$$g_1(E)=\frac{1}{k_BT_0}\exp\left(\frac{-E_1}{k_BT_0}\right)$$

$$\text{Relative decrease}=\frac{\int_{E_d^-=k_BT\ln\left(k_{-1}^0 t\right)-\Delta E}^{E_d^+=k_BT_w\ln\left(k_1^0 t_w\right)} g_1(E_1)\,dE_1}{\int_0^{E_d^+=k_BT_w\ln\left(k_1^0 t_w\right)} g_1(E_1)\,dE_1}=\frac{\left[\left(k_{-1}^0 t\right)^{-T/T_0}\exp\left(\frac{-\Delta E}{k_BT_0}\right)-\left(k_1^0 t_w\right)^{-T_w/T_0}\right]}{\left[1-\left(k_1^0 t_w\right)^{-T_w/T_0}\right]}=\frac{\exp\left(\frac{-E_d^- -\Delta E}{k_BT_0}\right)-1+\eta}{\eta}$$

III Basic experimental analysis of the relaxation

III.1 distribution function determination for the reverse reaction

For finding the distribution function when there is no ideas of the shape, one has to follow the same way as in section II2.

1) note:

$$\frac{d[B]}{dE_d} = -B_0(E_d)g(E_d)$$

2) with the assumptions II3AA,B (and even less i.e. assumption on first order reaction is not necessary)

$$[B](t,T) = \int_0^\infty (1 - x(E - E_d))B_0(E)g(E)dE \quad with \quad E_d = k_B T \ln(k_0 t)$$

we note that t, T are equivalent => equivalence between isotherms and isochrons

main problem: to find k_0

1) Measurement of several isochrons or isotherms (fig. 31 a-f)

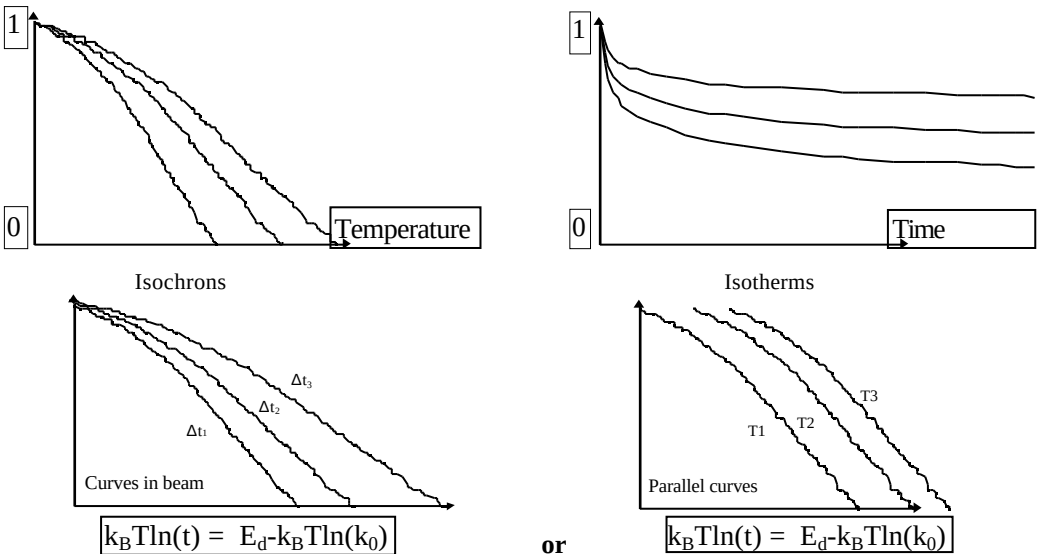

2) k_0 fitting

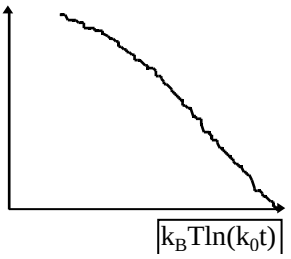

3) differentiation $\frac{d[B](t)}{dE_d} = -B_0 g_1(E_d(t))$

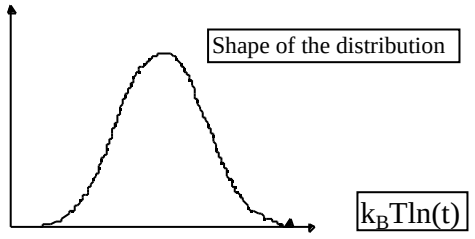

N.B. k_0 - g(E) separation

III.2 practice

The example we have chosen is the case of Bragg grating written in a tin doped optical fiber core. We make the assumption here that index change modulation is proportional to point index change (see section VI). Results are from P. Niay, M. Douay et al. [38]. Five isotherms are available that we can see in fig. 33 (79, 194, 299, 386°C, 500°C). The last isotherm is not recorded in the same conditions than the others (index change at the origin is 2.4 10^{-4} for 500°C whereas it is 2 10^{-4} for the others) but we will see that it is not so awkward.

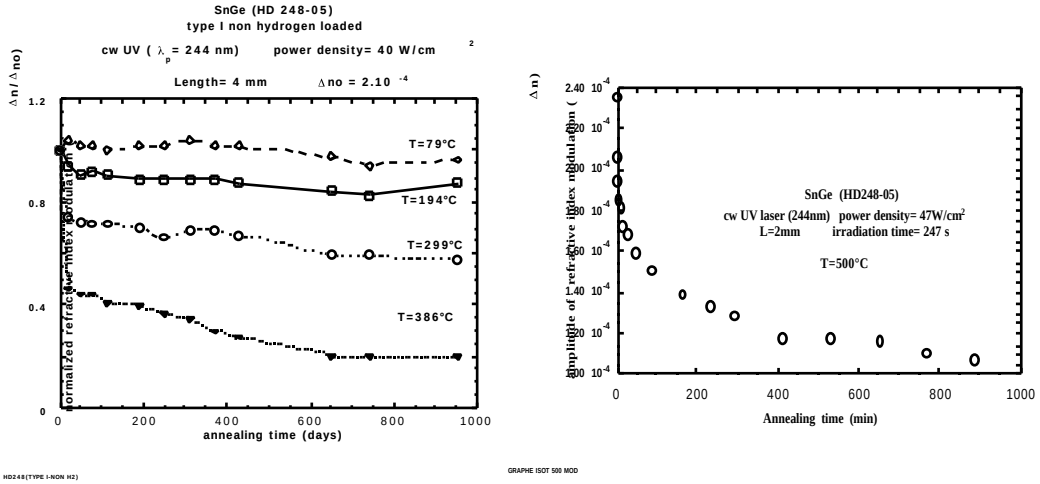

Fig. 33: a and b isotherms from P. Niay, M.Douay et al. [38]

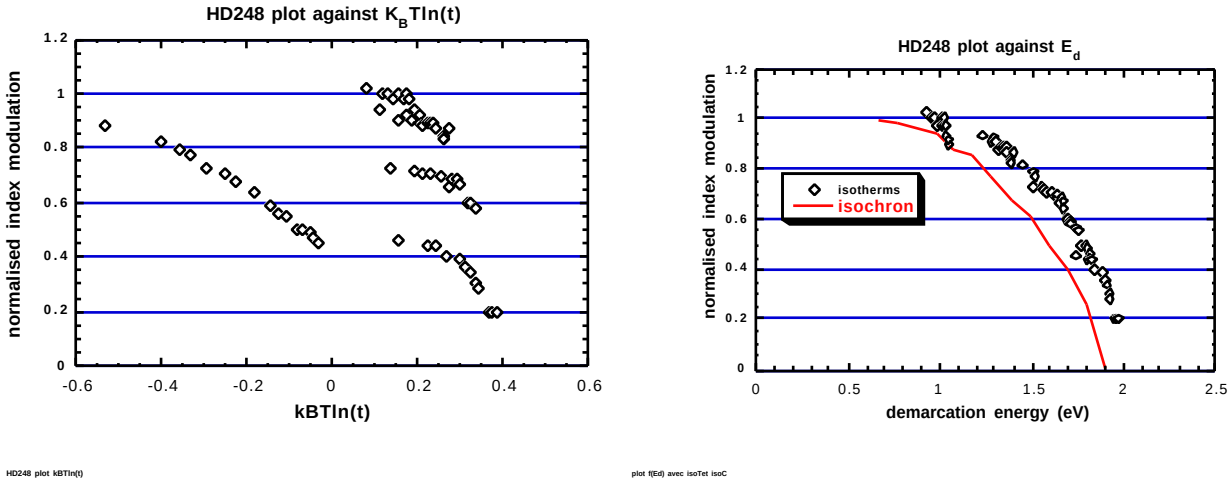

Fig. 34: Plot of results of fig. 33 against k_BTln(t). Fig. 35: Plot against demarcation energy, an isochron has been added.

After plotting against k_BTln(t), we obtain the fig. 34 which should show parts of parallel curves. We have to align these ones looking for the constant k_0. This can be made automatically by fitting of polynomial of demarcation energy k_BTln(k_0t). This has been made in fig. 35 yielding k_0=0.6 to 2.4 10^{12} day^{-1}. We can here check that it was possible to find a frequency factor so that the hypothesis of one order reaction for relaxation is fulfilled. Let us go on further to distribution determination. There are two solutions: one is to differentiate the fitted polynomial and try to fit a known expression that it is possible to find for instance in commercial soft. Here it seems realistic that the

distribution is a bell shape function and so an incomplete sigmoidal function appears suitable (see section II3D2). Fig. 36 shows the fit in full line of the expression below:

$$\frac{[B](t)}{B_1} = \frac{1-\left(k_0 t\right)^{-\frac{T}{T_0}} \exp\left(-\frac{E_0+\Delta E}{k_B T_0}\right)^{1-\eta}}{1+\left(k_0 t\right)^{-\frac{T}{T_0}} \exp\left(-\frac{E_0+\Delta E}{k_B T_0}\right)}$$

The gratings appears to be non saturated, written to 72%±10% in the sense that the index was not saturated (this has nothing to do with the reflectivity). The pre-exponential factor is 2.5 10^{-4}±30% and T_0=2670±200K. As we have seen in section III1 under validity of a few assumptions, there is a ln(t), T equivalence. The plot of an isochron in fig. 35 shows a shift which is explained by P. Niay et al. by different temperature of measurement of the reflectivity.

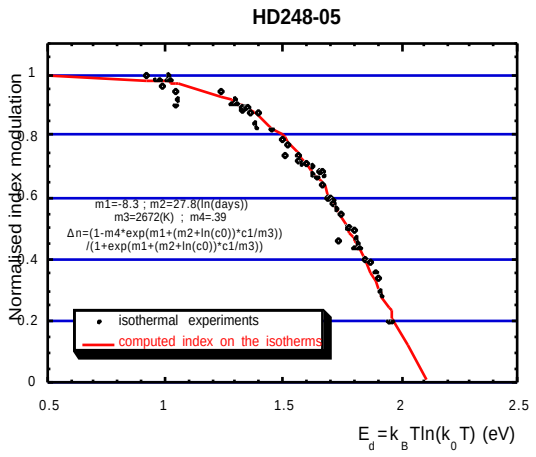

Fig. 36: η (the proportion to saturation of the gratings) is found at 72% ±10%, the rate constant for the stability is 1.2 10^{12} day^{-1} ±factor 2, the pre-exponential factor is 2.5 10^{-4}±30% and T_0=2670±200K.

III.3 stabilisation

Since the life function is now available, it is possible to stand that for a maximum specified temperature of T=273+40K and 25 years, the grating strength will decrease to .974.

It is also possible to study the stabilisation in order to increase the lifetime of our grating eventually. The principle is based on the distribution of B species stability at various sites. A burning in process suppresses the less stable sites. This cannot be achieved with an exponential kinetics.

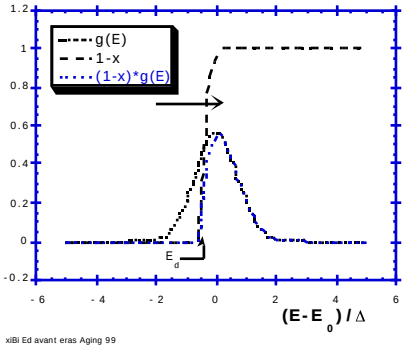

Fig. 37 Effect of an annealing on the B distribution: erase the less stable species

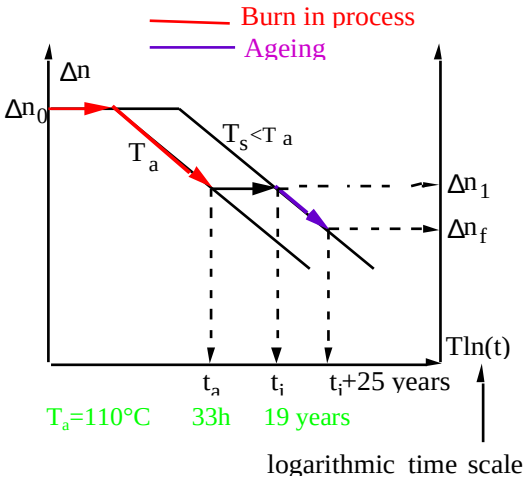

Fig. 38: Thermal stabilisation of Bragg gratings

The stabilisation induced by an annealing can be computing by renormalising the final value of the index change Δn_f after a time t at temperature T by the index change Δn_1 after burning in process. If we impose that after a given time at a given temperature (let us say 25 years at 40°C for instance), the ratio $\Delta n_f/\Delta n_1$ has to remain within a given range $1-\varepsilon < \frac{\Delta n_f}{\Delta n_1} < 1$ with ε<1% for instance, we obtain thus the duration and the temperature of strengthening of the grating. Using the data in figure [5], we got here, 33h, 110°C.

IV Peculiar properties in the frame of assumption validity

IV.1 writing-relaxation connection (A->B, B->A)

We have seen that it is interesting to write at the highest temperature because E_d increases on T and thus the stability also (see section II3D1). However, sometimes the reverse reaction (B->A) become active introducing a limitation.

For low or room temperature, we have noticed the following two cases:

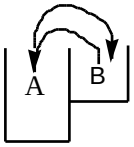

1) when the limiting reaction is the same in both sense, the distribution function is the same for forward and backward reaction. If the writing kinetics is not saturated, the forward distribution function is not saturated and so the backward distribution neither. The stability is dependent on the writing ($B_0(E)$) see section II3D

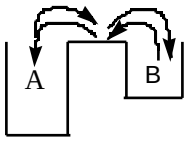

2) when there is no correlation between the distribution functions. The B sites are randomly occupied whatever the depth. The complete distribution function of the backward reaction has to be used.

The stability is independent of writing (i.e. on the initial grating strength) see section II3C.

Fig. 39:

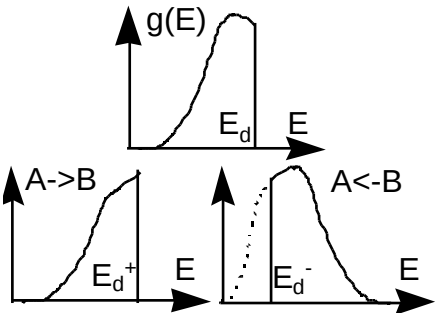

Fig. 40:

For high T, an equilibrium is developed in both cases because the reverse reaction cannot be neglected anymore.

1) case 1 (same pathways): we will show that the distribution function is cut at large E_d at more elevated temperature. Stability increases because more stable sites are filled [37] (see section A below).

2) case 2 (different pathways, two distribution functions): stability increases because less stable sites are removed in the reverse distribution function during writing (section B below).

A) Writing in the case of reversible reaction

The equations applicable in the case of reversible kinetics, are written below. Now, the degree of advancement x_1 will never reach 1 but will remain limited by the rate k_1^0 / k_T^0.

$$A \underset{k_{-1}}{\overset{k_1}{\rightleftharpoons}} B \quad x_1(E_1, T) = \frac{k_1^0}{k_T^0}\left(1 - \exp\left(-k_T t\right)\right)$$

$$with \quad k_T^0(T) = k_1^0 + k_{-1}^0 \exp\left(-\frac{\Delta E}{k_B T}\right)$$

Using the same procedure as in section II2C, the integral of B is solved with a new expression for the demarcation energy including the total rate constant in the E_1 scale ($k_T^0(T)$, $E_d = k_B T \ln\left(k_T^0(T)\, t\right)$ see [37]. Using distribution from differentiation of a sigmoid, we get the following expression:

$$[B](t) = A_0 \frac{k_1^0}{k_T^0} \frac{\left(k_T^0(T)t\right)^{\frac{T}{T_0}} \exp\left(-\frac{E_0}{k_B T_0}\right)}{1 + \left(k_T^0(T)t\right)^{\frac{T}{T_0}} \exp\left(-\frac{E_0}{k_B T_0}\right)} \qquad \alpha = \frac{T}{T_0}$$

$$a = \exp\left(\frac{T}{T_0}\ln\left(k_T^0(T)\right) - \frac{E_0}{k_B T_0}\right)$$

The expression of $[B](t)$, reveals that power law with the same exponent as in section II is still followed but pre-exponential factor is modified. Now, the dependence of the pre-exponential factor (a), is super-exponential. It is due to the variation of total rate constant with temperature. The growth of index during writing will be faster at higher temperature but limited to k_1^0 / k_T^0 which itself decreases on temperature. There is so a compromise.

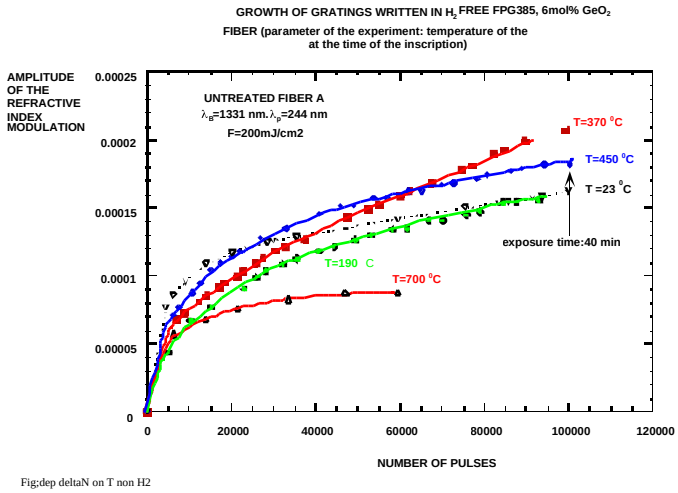

Fig. 41: results from Bernage et al. [4]

E_d is no more proportional to T and so it is no more possible to find a k_0 with isochronous experiments. Two parameters are necessary. The ln(t), T equivalence is broken.

Example (reversible)

This is an example from P. Bernage et al. [4], we can see that the reverse reaction becomes predominant at high temperature (fig. 41).

B) erasure in the case of reversible reaction

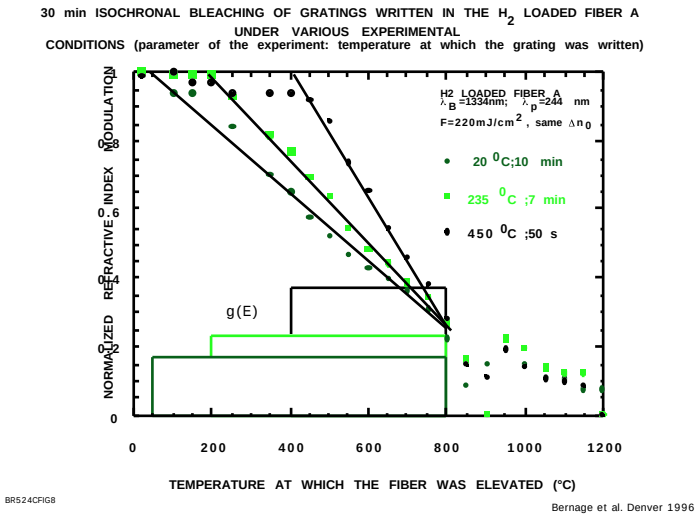

Fig. 42: Stability of gratings written with the same Δn_0 but at different temperature.

In this case, only the backward reaction $A \overset{k_{-1}}{\leftarrow} B$ is active because forward rate is nulled when light power density is zero. The expression for $\frac{[B](t)}{B_0}$ is the same in replacing k_1^0 by k_T^0 in corresponding expression for stability. Conclusions are thus the same as in previous section except temperature dependence is a little more complex.

C) Stability when forward and backward reactions are independent

How to interpret the results in fig. 42 It is stability of Bragg gratings written at different temperature in a H_2 loaded fibers. It is increasing as the writing temperature increases. The distribution function of the backward reaction is a top hat function since in this isochronous plot the curve is linear

from ordinate 1 (results above 800°C are relevant of a second mechanism that we forget here). the distribution function for the forward reaction is probably a bell shape curve when power law is detected or more complex as two successive reactions are pointed out (see section V3). Forward and backward distribution are independent since stability of gratings written with different strength but at the same temperature exhibit the same stability [39].

During the writing at room temperature there is only reaction $A \rightarrow B$ working, the square distribution lies from room T to 800°C. At writing temperature of 235°C, it needs less time to reach the same index change because writing reaction is thermally activated. On the other hand, the reverse reaction is also thermally activated and bleached a part of the result of the forward reaction, the less stable sites. Therefore, the distribution function is "eaten" on the low energy side. As the distribution integral area should remain constant, its intensity increases.

E) Writing in the case of independent forward and backward reactions

The resolution in this case is not obvious. Let us see only that the equations are as follows:

$$A \underset{k_{-1}}{\overset{k_1}{\rightleftharpoons}} B \qquad x_1\left(E_1, E_{-1}, T\right) = \frac{k_1}{k_T}\left(1 - \exp\left(-k_T t\right)\right)$$

with $k_T = k_1 + k_{-1}$

$$B(t,T) = \int_0^\infty \int_0^\infty g_+\left(E_+\right) g_-\left(E_-\right) \frac{k_1\left(E_+\right)}{k_T\left(E_+, E_-\right)} \left(1 - \exp\left(-k_T\left(E_+, E_-\right)\right)\right) dE_+ dE_-$$

IV.2 isotherm-isochron equivalence

Before to compare isochrons and isotherms it is necessary to be sure that the various measurements have been achieved at the same temperature let us say at room temperature. This means that the grating is quenched at room temperature after annealing at another temperature. This problem has been addressed extensively by Razafimahatratra et al. [40].

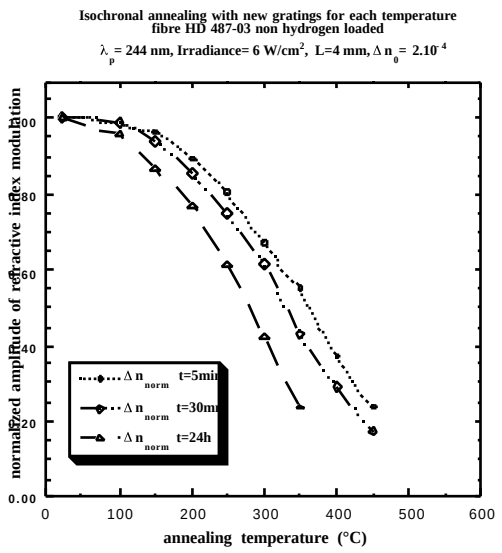

isochrones reseaux vierges

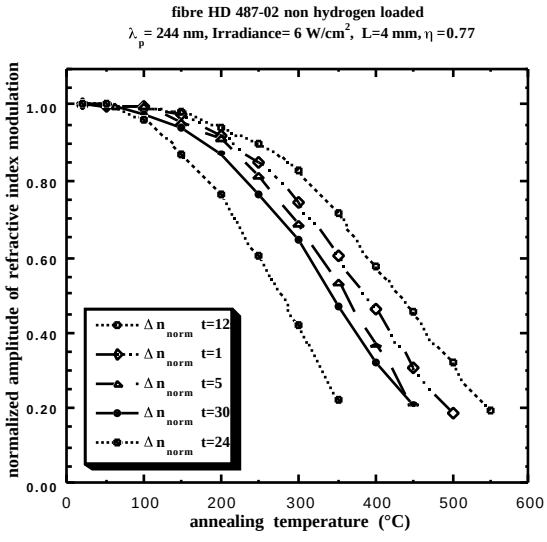

isochrone classique

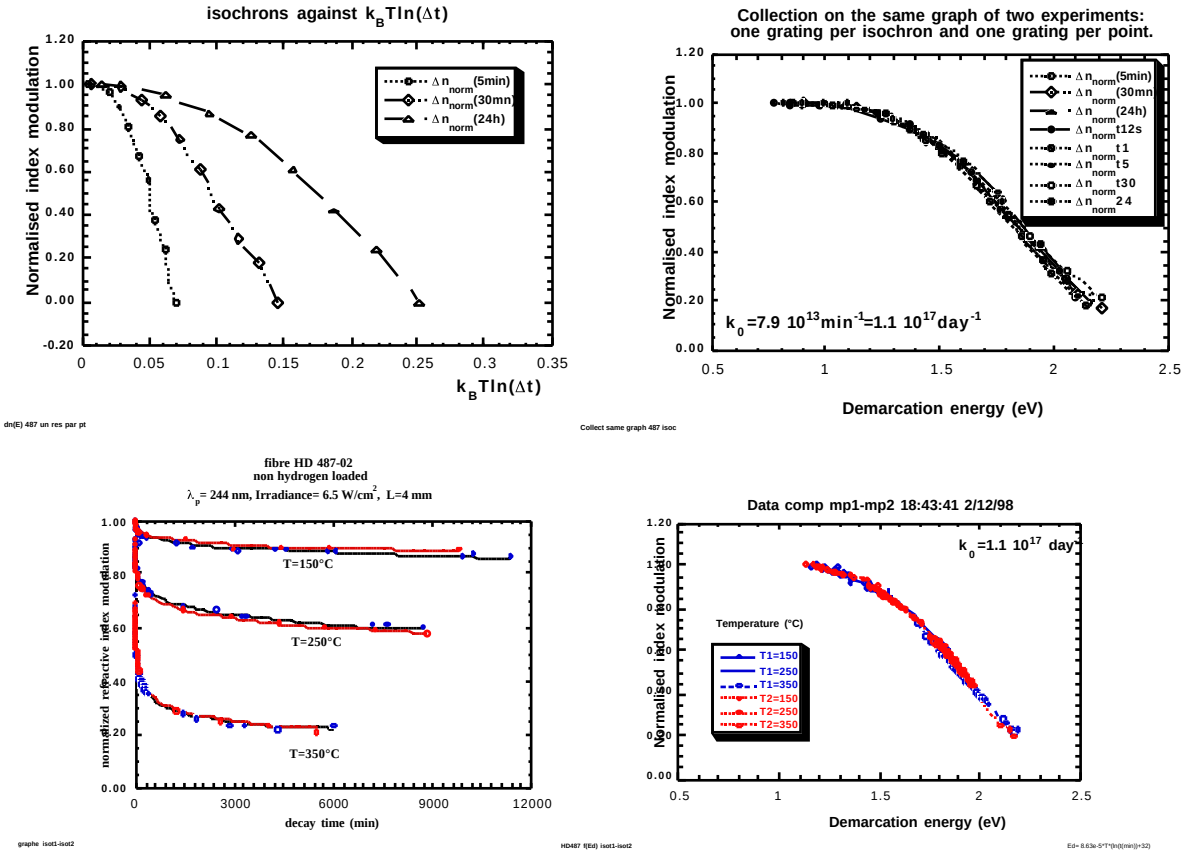

Fig.43: Set of isochrons and isotherm obtained by [40] a and b compare isochrons obtained on one hand and from one grating for each temperature and another one with one gratings by isochrons. C is the curve beam obtained after replotting as mentioned in section III1. d is the master curve deduced for the isochrons. e-f is isotherm experiment. The same master curve is obtained after correction of the temperature of measurement.

A second problem is that the step isochrons have been performed correctly, i.e. that the step of the isochrons are independent. This is achieved is the condition $\left(\delta t.k_0\right)^{-\frac{\Delta T}{T_{\max}}} << 1$ where δt is the duration of the step annealing, ΔT is the temperature step increase, T_{max} is the maximum temperature achieved on the isochrons. In that case, taken a new grating for each isochrons or use the same grating step by step is equivalent as it is shown in the figure 43 a-d. From the simple theory, $\Delta n=f(E_d)$, $E_d=k_B T\ln(k_0 t)$ <=> t,T equivalence

Relevant assumptions: - the distribution function is not T dependent,

- only one limiting reaction

Finally; it is possible to plot all results on the same plot using a demarcation and a suitable k_0 quantity, here we have used k_0= 1.1 10^{17} day^{-1}. Using the same k_0 constant, it is also possible to rescale the isotherms and to superimpose isochrons and isotherms. This shows that the simple approach is applicable.

Example of equivalence breaking

ex 1: non T dependent distribution against T dependent one

-Riant et al. [5]: non T dependent top hat function.

$$\frac{\Delta n}{\Delta n_0} = 1 - \frac{E_d - E_{\min}}{E_{\max} - E_{\min}}, \quad g(E) = \begin{cases} 0, E < E_{\min} \\ \dfrac{1}{E_{\max} - E_{\min}}, E_{\min} < E < E_{\max} \\ 0, E_{\max} < E \end{cases}$$

-Baker et al. [41]: T dependent top hat function

$$\frac{\Delta n}{\Delta n_0} = 1 - \frac{E_d - E_{\min}}{Ak_BT}, \quad g(E) = \begin{cases} 0, E < E_{\min} \\ \dfrac{1}{Ak_BT}, E_{\min} < E < E_{\min} + Ak_BT \\ 0, E_{\min} + Ak_BT < E \end{cases}$$

These two interpretation can be differentiated comparing isochrons and isotherms, there is t,T equivalence in the first case and non t,T equivalence in the second case.

ex2: occurrence of a secondary reaction

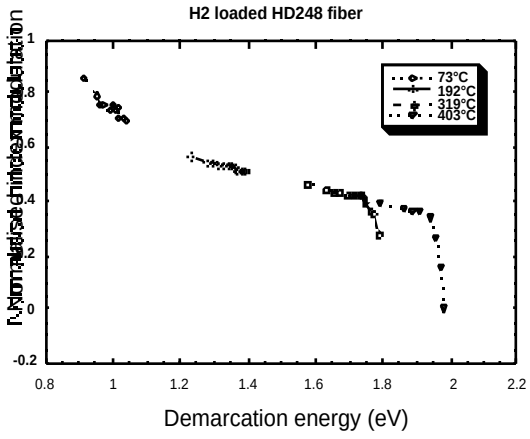

Fig. 44 Result from [40]

In the chosen experiment, RIC is achieved by a 248 nm pulsed laser after H_2 loading at low T high P. The isothermal measurements on a very long period (3 years) have been plotted according to the demarcation energy with a rate constant of 1.4 10^12 day-1. The distribution curve which can be obtained by differentiation of the plotted curve for E<1.7 eV is here closer to a decreasing exponential. The drops at the end of the plot are relevant of another reaction with a much smaller rate constant (90 day-1, (Razafimahatratra et al. To be submitted)).

The figure in the case of highly Ge doped fiber core shows that it is not possible to obtain a complete master curve due to another process occurring at the end of high temperature treatment. There are two reactions, two Ed's are required and simple theory is not applicable (see section V.2)

IV.3 k_0 comparison

We have seen before that it is possible to get a Master curve providing only one parameter i.e. k_0 when suitable assumption are fulfilled.

After obtaining k_0 and master curve, we can compare the different stability functions (fig. 45). It is not necessary for that purpose to have a functional of E_d for performing this comparison but only the assumption of only one reaction active.

We can observe that the energies lie in the same range. This is due to observable property. The shapes of the curves are different arising from different distribution function. $k_{0's}$ however are quite different. Weight effect of vibrating species is not enough for explaining the observed range (as it is usual in solid). It is the probability for a cluster formation: the "transient complex". The larger the complex, the smaller the probability. Other examples can be found

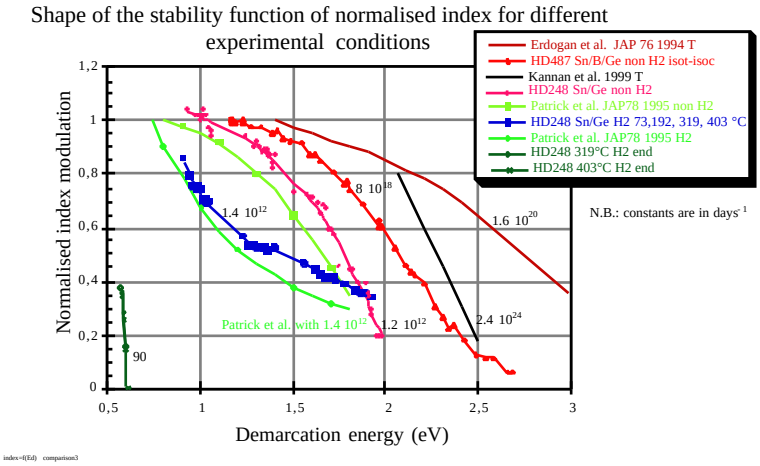

Fig. 45: Comparison of stability between various cases.

in Chabrerie, showing that it can depends on the effective trapping cross section with a T^2 dependence eventually. In any case, k_0 is an information on the B trapping mechanism in its potential well.

V Beyond simple theory

V.1 higher order reaction

This problem has been already mentioned by Primak [30]

$$A \xleftrightarrow{k} 2B, \quad k = k_0 \exp\left(-\frac{E}{k_B T}\right)$$

$$\frac{dx}{dt} = k(E)x(E,t)^2$$

$x(E,t) = \dfrac{1}{1+\dfrac{1}{B_0 t k_0 \exp\left(-\dfrac{E}{k_B T}\right)}}$ defining E_d with x(E,t)=1/2, we get if B_0 does not depend on E and

$x(E,t) = \dfrac{1}{1+\exp\left(\dfrac{E-E_d}{k_B T}\right)}$ which can be considered as rapidly varying on E.

Then $B_T = B_0 \int_0^\infty x(E,t)g(E)dE$ and $B_T = B_0 \int_{E_d}^\infty g(E)dE$ as for first order but with $E_d = k_B T \ln(B_0 k_0 T)$. The reaction properties are in E_d and the disorder in g(E). But E_d depends on B_0 i.e. on the grating strength. The main conclusion is that stability depends here on the grating strength even if forward and backward reaction are independent.

V.2 two parallel reactions

Below are experimental results from Razafimhatratra et al. [40] in the case of H_2 loaded fiber (fig. 46). A first k_0 can be found collapsing the curve at low t and low T (fig. 47). These master curves have been obtained with a rate constant equal to 1.4 10^{12} day^{-1}. Another k_0 can be obtained when collapsing curves at large time or high temperature.

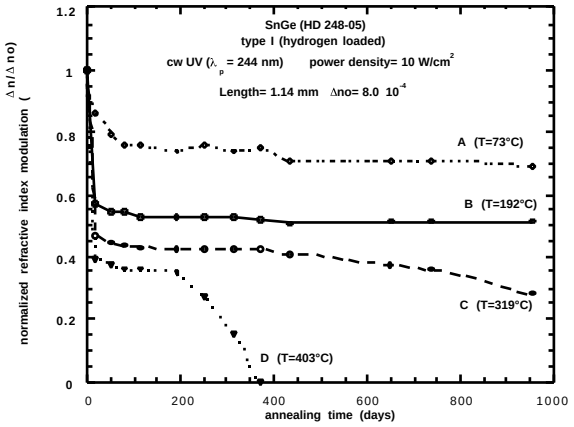

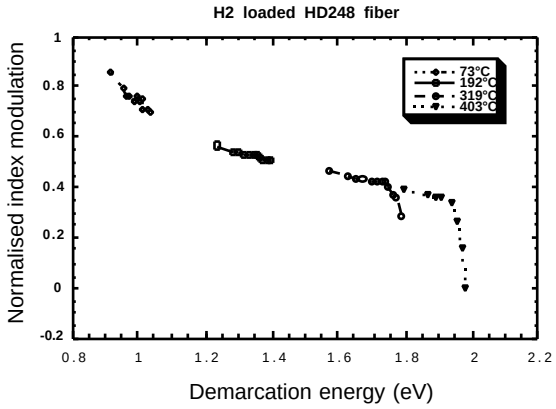

Fig. 46: Results from [40] and Fig. 47: Corresponding master curve for low t and T.

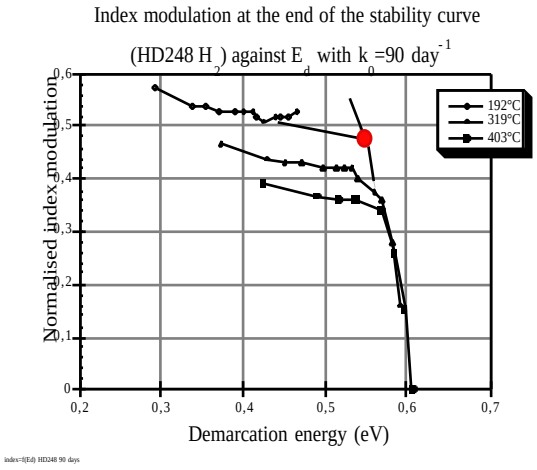

Fig. 48 The second master curve for large t and T.

Theory of serial reactions

Theory

$$A_1 \xleftarrow{k_1} B \qquad A_2 \xleftarrow{k_2}$$

$$\frac{d\eta}{dt} = -\left(k_1(E_1) + k_2(E_2)\right)\eta$$

$$\eta(E_1, E_2, t) = \exp\left[-\left(k_1(E_1) + k_2(E_2)\right)t\right]$$

$$\frac{[B](t)}{B_0} = \int_0^\infty\int_0^\infty \exp\left[-\left(k_1(E_1) + k_2(E_2)\right)t\right] g(E_1) g(E_2)\, dE_1 dE_2$$

$$\frac{[B](t)}{B_0} = \int_0^\infty \exp\left[-k_1(E_1)t\right] g(E_1) dE_1 \int_0^\infty \exp\left[-k_2(E_2)t\right] g(E_2) dE_2$$

$$\frac{[B](t)}{B_0} = \int_{E_{d,1}=k_BT\ln(k_{0,1}t)}^\infty g(E_1) dE_1 . \int_{E_{d,2}=k_BT\ln(k_{0,2}t)}^\infty g(E_2) dE_2$$

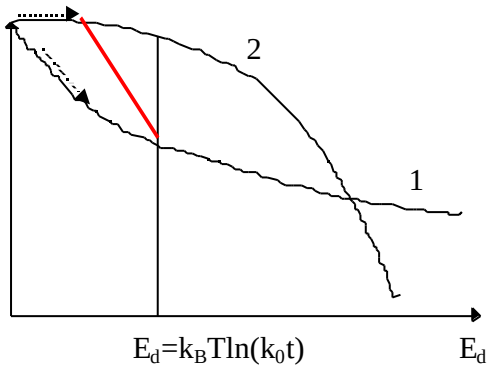

$k_{02} << k_{01}$

$E_{d,1} > E_{d,2}$

Fig. 49 a Due to different k_0, the rate of evolution along reaction 1 or 2 are not the same.

We note by the way that isotherms and isochrons are again no more equivalent. Let us illustrate the complex behaviour of B. We have chosen the constant rate $k_{0,2}$ smaller than $k_{0,1}$. In this case $f(E_{d,1})$ and $f(E_{d,2})$ are different for a given t,T couple. $E_{d,1}$ and $E_{d,2}$ have not the same value (fig. 49a).

In a ln(t) plot, the stability curves are shifted from each other (fig. 49b). The fastest reactions are predominant (curve 1) and we see almost only the curve 1 behaviour in the physical quantity. For large T, the second behaviour appears. At larger T, the curve 1 is shifted more left handed and the curve 1 behaviour is even more predominant in the behaviour of the final physical quantity (fig. 49c). At large t, curve 2 behaviour appears but for a smaller contribution.

Isothermal description

$k_{02}<<k_{01}$

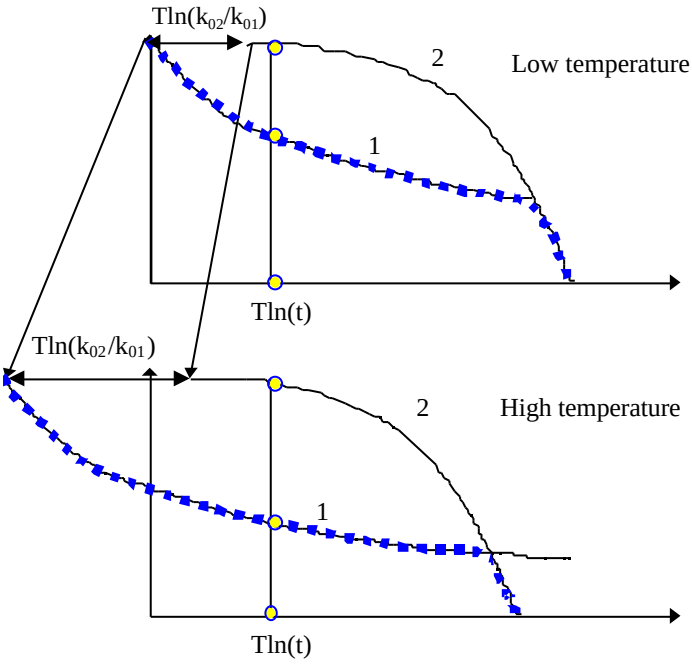

Fig. 49 b and c: Isothermal description. The dashed line shows the evolution of the erasure.

Along the isochronal curves in fig. 49d, the temperature changes and the shift between curve 1 and 2 is increased in such a way that process 1 may have erased grating before process 2 appears. This may lead to error on isothermal life time estimate.

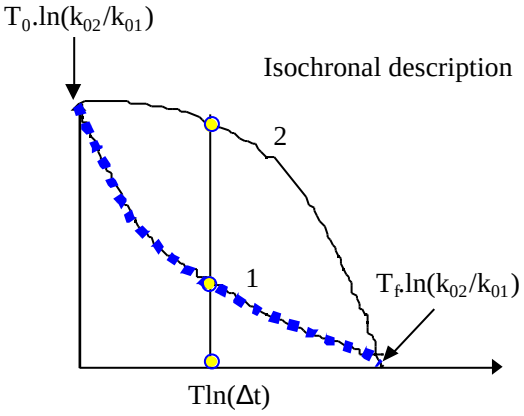

Fig. 49d Isochronal description. Since the shift of the master curves increases as T increases, the cross point can be not detectable.

V.3 serial reactions

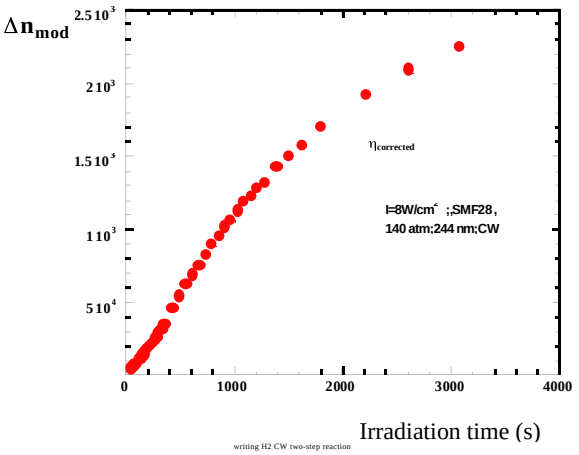

Fig. 50: Index change in H_2 loaded SMF28 (Corning) during writing with a CW 244 nm laser [42].

Example of serial reactions can be found in different fields like quasi elastic neutron scattering in PVC [43] or E' center production under X-ray in SiO_2 [44] but I will stay in our field considering the index change during writing after H_2 loading. In this case, a sigmoidal curve is recorded according to the fluence (fig. 50 showing the occurrence of two serial reactions [42]).

Theory of serial reactions

site under construction

V.4 narrow and steep distribution function

The approximation of demarcation energy is based on the condition that the distribution function varies slower than x(E,t) (see section II2). In the contrary case, it is no longer valid. Especially, it is not directly applicable for a Dirac distribution function (SIREPA for single reaction pathway). However, it is possible to show that the approach can be extended considering an experimental distribution function which is the actual one convoluted by the derivative of the advancement degree.

Here is the demonstration

1) if I look for the experimental distribution by differentiation of B versus the demarcation energy in considering that it is possible to write X(E,t,T)=X(E-E_d), I get $B = \int_0^\infty g(E)X(E - E_d)dE$. Then I get the following:

$$\frac{dB}{dE_d} = \int_0^\infty g(E)\frac{d\left[X\left(E - E_d\right)\right]}{dE_d}dE = -\int_0^\infty g(E)\frac{dX}{dE}\Big|_{E-E_d} dE = \underbrace{\left[g * \left(-\frac{dX}{dE}\right)\right]_{E_d}}_{= \tilde{g}\left(E_d\right)}$$

the experimental distribution is the theoretical distribution broadened by dX/dE

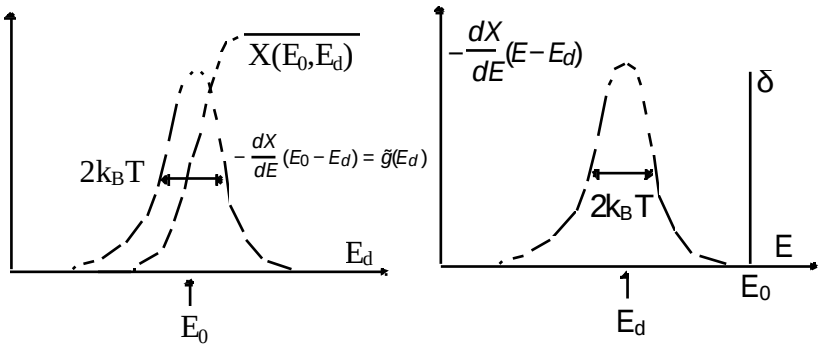

Fig. 50: Derivative of the reaction advancement degree.

In particular, the Dirac function for simple exponential will appear as a narrow bell shape curve of width 2kT.

$$\underbrace{\tilde{g}(E)}_{\text{experimental distribution function}} = \underbrace{g \otimes \left(-\frac{dX}{dE}\right)}_{\substack{\text{theoretical distribution function} \\ \text{experimental distribution is the theoretical one broadened by } \frac{dX}{dE} \\ width = 2k_BT}} \quad \text{where } X(E_d) = 1 - \exp\left(-\exp\left(\frac{E_d - E_0}{k_BT}\right)\right)$$

2) inverse problem (to find the analytical function for B)

If we consider $\left[g \otimes \left(-\frac{dX}{dE}\right)\right]_{E_d} = \tilde{g}(E)$ and I use the cutting method for computing the integral B i.e. $B(E_d(t)) = \int_0^{E_d(t)} \tilde{g}(E)dE$. Am I going to find $B(t) = \int_0^{\infty} g(E)x(E,t)dE$? In fact, we get the following:

$$B(E_d) = \int_0^{E_d} \tilde{g}(E)dE = \int_0^{\infty} g(E)X(E-E_d)dE - \underbrace{\int_0^{\infty} g(E)X(E)dE}_{\substack{\approx 0 \text{ if the distribution does} \\ \text{not touch zero energy.}}}$$ i.e. just what we were looking for.

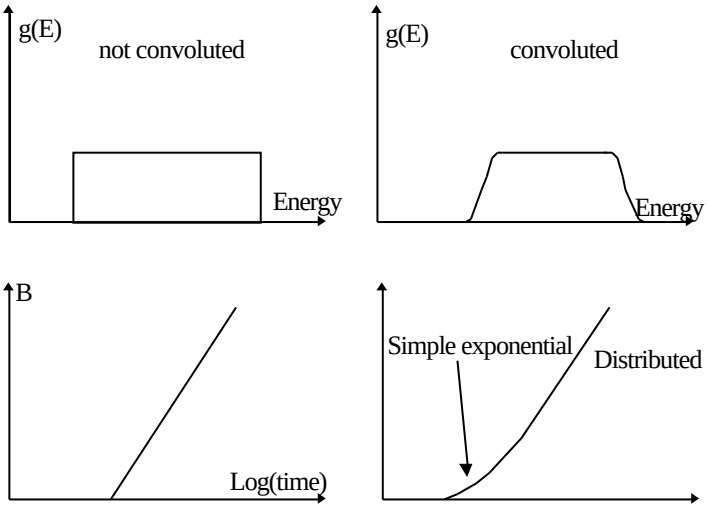

Fig. 48: Effective distribution function.

In conclusion, VAREPA approach can be applied to any distribution performing at the end a deconvolution. For instance, in the case of a square distribution (fig;48) like when the low Ge doped fiber is hydrogen loaded, the edge of the distribution will be smoothed giving rise at the beginning of the reaction to a simple exponential behaviour on time.

V.5 distributed non activated kinetics (photochromism, luminescence)

The equation of excitation is the following one: $\frac{dA^*}{dt} = \varepsilon(h\nu)AP/h\nu$, we can note that if $\varepsilon(h\nu)$ the molar absorptivity is varying rapidly on $h\nu$ (edge absorption), we can use the VAREPA approach to compute the excited state concentration. The erasure corresponds to luminescence if the stability of luminescence site is distributed, the lifetime will increase on time.

VI Real analysis of Bragg grating writing and stability

In analysis of the index change deduced from Bragg gratings, we have to pay attention that we work on index modulation and average but not on point index change. However, all theory developed above is for point index change. the difference between this two quantities is Fourier transform along z i.e. along Power density fluctuations. To make the link between them, it is therefore necessary to know the relation between k_0t and P. Is k_0 proportional to P or to P^2?

Of course, non linear dependence on P combined with the non-linear behaviour on k_0t will lead to distortion of interference pattern and to bandwidth broadening.

But, it is not the only detrimental effect. Recalling the conclusion of section II3D, the stability of interfrange will be smaller than the one at the max in the fringe. Therefore, during a burning in process, in non H_2 loading fibers made by pulsed laser (for instance) can exhibit a broadening.

VII Practical formalism to describe generalised thermally activated processes.

Let us mention here that a general approach applicable to any activation energy processes analysed by any experimental measurements (isothermal, isochronous or tempering) has been published by Miller et al.[33]. These authors demonstrate a numerical solving of the generalised equation in which k_0, T, or the energy reference can be time dependent. They use again a cutting energy which is defined by $\left.\frac{\partial^2 x}{\partial E \partial t}\right|_{E=E_d} = 0$.

Specifically, for tempering, the demarcation energy is defined by an expression quite different than for isothermal experiments.

$$\frac{E_d}{k_B T} + \ln\left(\frac{E_d}{k_B T}\right) + 2 = \ln\left(k_0 c k_B T\right) \text{ where c is defined by } T(t) = \frac{t}{c k_B} + T_0 \qquad [45]$$

VIII Conclusion

We have shown a development of a framework for modelling the relaxation behaviour of UV induced refractive index change based on distributed activation energy of a physico-chemical reaction. From experimental measurements (isochrons and isotherms), this framework allows to find the distribution function providing only a constant which can be determined by simple variable change when a few assumption are verified. From this distribution, it is possible to know the complete time behaviour and to determine the annealing conditions for extending the lifetime.

This approach can be used for other physical quantities, e.g. photodarkening, stress relaxation, luminescence decay.

Finally, let us mention that the formalism developed here for time evolution of an activated energy process can be used for analysing frequency behaviour of similar system. For instance, Perlmutter et al. describes quasielastic light-scattering spectrum analysis in the range 0.1 to 100 Mhz in term of energy barrier distribution of sites similar to a Poisson one. The analogue demarcation energy is here $kT\ln(k_0/\omega)$.

Acknowledgements

I am very grateful to Profs. P. Niay, M. Douay for many discussions and the availability of their measurements. I thank you also Dr Chabrerie for his important thesis.

references

[1] T. Erdogan, V. Mizrahi, P. J. Lemaire, and D. Monroe, "Decay of ultraviolet-induced fiber Bragg gratings.," *J. Appl. Phys.*, vol. 76, pp. 73-80, 1994.

[2] S. Ishikawa, A. I. Inoue, and M. Harumoto, presented at OFC 98, 1998.

[3] R. Richert and A. Blumen, "Disorder effects on relaxational processes.," : Springer Verlag, 1994.

[4] P. Bernage, T. Taunay, B. Leconte, M. Douay, P. Niay, J. F. Bayon, H. Poignant, H. Herlemont, J. Legrand, and B. Poumellec, "Inscription kinetics and thermal stability of Bragg gratings written within heated fibers.," presented at Doped Fiber Devices and systems II, Denver, Colorado, USA, 1996.

[5] I. Riant and B. Poumellec, "Thermal decay of gratings written in hydrogen-loaded germanosilicate fibers.," *Electronics Letters*, vol. 34, pp. 1603-1604, 1998.

[6] W. X. Xie, P. Niay, P. Bernage, M. Douay, T. Taunay, J. F. Bayon, E. Delevaque, and M. Monnerie, "Photoinscription of Bragg gratings within preform plates of high NA germanosilicate fibers: Searching for an experimental evidence of type II A photosensitivity in preform plates," *Optics Communications*, vol. 124, pp. 295-300, 1996.

[7] W. X. Xie, P. Niay, P. Bernage, M. Douay, T. Taunay, J. F. Bayon, E. Delevaque, and M. Monnerie, "Photoinscription of Bragg gratings within preform plates of high NA germanosilicate fibers: Searching for an experimental evidence of type II A photosensitivity in preform plates," *Optics Communications*, vol. 124, pp. 295-300, 1996.

[8] B. Poumellec, P. Niay, M. Douay, and J. F. Bayon, "The UV induced refractive index grating in Ge-SiO_2 preforms: additional CW experiments and the macroscopic origin of the change in index.," *Journal of Physics D: Applied Physics*, vol. 29, pp. 1842-1856, 1996.

[9] C. Fiori and R. A. B. Devine, "Ultraviolet irradiation induced compaction and photoetching in amorphous, thermal SiO_2.," presented at Mat. Res. Soc. Symp., 1986.

[10] W. Primak and R. Kampwirth, "The radiation compaction of vitreous silica.," *Journal of Applied Physics*, vol. 39, pp. 5651-5658, 1968.

[11] C. A. Allan, C. Smith, N. F. Borelli, and T. P. S. III, "193-nm excimer laser induced densification of fused silica.," *Optics Letters*, vol. 21, pp. 1960-1962, 1996.

[12] P. J. Lemaire, "Reliability of optical fibers exposed to hydrogen: prediction of long-term loss increases.," *Optical engineering*, vol. 30, pp. 780-789, 1991.

[13] J. F. Marcerou, H. Février, P. M. Gabla, and J. Augé, "Sensitivity of erbium-doped fibers to hydrogen: implications for long-term system performance.," presented at Optical Fiber Communication'94, San Jose, California, USA, 1994.

[14] Rush, *British Telecom Technology*, 1984.

[15] C. L. Smith, "A theory of transient creep in metals.," *The proceedings of the physical society.*, vol. 61, pp. 201-205, 1948.

[16] M. Poirier, S. Thibault, J. Lauzon, and F. Ouellette, "Dynamics and orientational behaviour of U.V. induced luminescence bleaching in Ge-doped silica optical fiber," *Optics Letters*, vol. 18, pp. 870, 1993.

[17] T. Erdogan, V. Mizrahi, P. J. Lemaire, and D. Monroe, "Decay of U.V. -induced fiber Bragg gratings," presented at Optical Fiber Communication'94, San Jose, California, USA, 1994.

[18] T. Erdogan, V. Mizrahi, P. J. Lemaire, and D. Monroe, "Decay of ultraviolet-induced fiber Bragg gratings.," *J. Appl. Phys.*, vol. 76, pp. 73-80, 1994.

[19] J. H. Kyung and N. M. Lawandy, "Direct observation of the effective $\chi^{(2)}$ grating in bulk glasses encoded for second-harmonic generation.," *Optics Letters*, vol. 21, pp. 632-634, 1996.

[20] E. J. Friebele, M. E. Gingerich, and D. L. Griscom, "Survivability of optical fibers in space.," presented at Optical Materials reliability and testing, 1992.

[21] V. D. Rodriguez, U. R. Rodriguez-Mendoza, I. R. Martin, V. Lavin, and P. Nunez, "Site distribution in Cr^{3+} and Cr^{3+}-Tm^{3+} doped alkaline silicate glasses.," presented at SiO_2 and advanced dielectrics., L'Aquila, Italy, 1997.

[22] O. Deparis, D. L. Griscom, P. Mégret, M. Decréton, and M. Blondel, "Influence of the cladding thickness on the evolution of the NbOHC band in optical fibers exposed to gamma radiations.," *Journal of Non-Crystalline Solids.*, vol. 216, pp. 124-128, 1996.

[23] D. Monroe and M. A. Kastner, "Exactly exponential band tail in a glassy semiconductor.," *Physical Review B*, vol. 33, pp. 8881-8884, 1986.

[24] M. Kroide, *Physics and chemistry of Glasses*, vol. 38, pp. 83-86, 1997.

[25] J. C. Phillips, "Kohlrausch relaxation and glass transitions in experiment and in molecular dynamics simulations.," *Journal of Non-Crystalline Solids*, vol. 182, pp. 155-161, 1995.

[26] Y. Mohanna, J.-M. Saugrain, J.-C. Rousseau, and P. Ledoux, "Relaxation of internal stresses in optical fibers.," *Journal of Lightwave Technology*, vol. 8, pp. 1799-1802, 1990.

[27] P. J. Lemaire and A. Tomita, "Behavior of single mode MCVD fibers exposed to hydrogen.," presented at European Conference on Optical Communications, Stuttgard, 1984.

[28] R. Kohlrausch, "Ueber das Dellmann'sche Elektrometer.," *Ann. Phys. (Leipzig)*, vol. 72, pp. 353-405, 1847.

[29] V. Vand, "A theory of the irreversible electrical resistance changes of metallic films evaporated in vacuum.," *Proceedings of Physical Society of London*, vol. A55, pp. 222-246, 1943.

[30] W. Primak, "Kinetics of Processes distributed in activation energy.," *Physical Review B*, vol. 100, pp. 1677-1689, 1955.

[31] W. Primak, "Large temperature range annealing," *Journal of Applied Physics*, vol. 31, pp. 1524, 1960.

[32] J. Orenstein and M. Kastner, "Photocurrent transient spectroscopy: measurement of the density of localized states in a-AS_2Se_3.," *Physical Review Letters*, vol. 46, pp. 1421-1424, 1981.

[33] S. L. Miller, P. J. McWhorter, W. M. Miller, and P. V. Dressendorfer, "A practical predictive formalism to describe generalised activated physical processes.," *Journal of Applied Physics.*, vol. 70, pp. 4555-4568, 1991.

[34] P. J. Lemaire, D. P. Monroe, and H. A. Watson, "Hydrogen-induced-loss increases in erbium-doped amplifier fibers: revised predictions.," presented at Optical Fiber Communication'94, San Jose, California, USA, 1994.

[35] J. P. Vandenbrink, "Master stress relaxation function of silica glasses.," *Journal of Non - Crystalline Solids*, vol. 196, pp. 210-215, 1996.

[36] S. Kannan, P. J. Lemaire, J. Guo, and M. J. LuValle, "Reliability predictions on fiber gratings through alternate methods.," presented at Bragg gratings photosensitivity, and poling in glass fibers and waveguides: applications and fundamentals., Williamsburg, Virginia, USA, 1997.

[37] B. Poumellec, “Links between writing and erasure (or stability) of Bragg gratings in disordered media.,” *Journal of Non-Crystalline Solids*, vol. 239, pp. 108-115, 1998.
[38] D. Razafimahatratra, “Etude de la stabilité de la variation d'indice de réfraction photoinduite par insolation laser dans les guides d'onde optiques germanosilicates.,” : University of Sciences and Technologies of Lille, 2000.
[39] H. Patrick and S. L. Gilbert, “Growth of Bragg gratings produced by continuous-wave ultraviolet light in optical fiber.,” *Optics Letters*, vol. 18, pp. 1494, 1993.
[40] D. Razafimahatratra, P. Niay, M. Douay, B. Poumellec, and I. Riant, “Comparison of isochronal and isothermal decays of Bragg gratings written through continuous-wave exposure of an unloaded germanosilicate fiber.,” *Applied Optics*, vol. 39, pp. 1924-1933, 2000.
[41] S. R. Baker, H. N. Rourke, V. Baker, and D. Goodchild, “Thermal decay of fiber Bragg gratings written in Boron and Germanium codoped silica fiber.,” *Journal of Lightwave Technology*, vol. 15, pp. 1470-1477, 1997.
[42] D. Ramecourt, P. Niay, P. Bernage, I. Riant, and M. Douay, “Growth of strength in H_2 loaded telecommunication fiber during CW UV post-exposure.,” *Electronics Letters*, vol. 35, pp. 329-330, 1999.
[43] K. L. Ngai, C. M. Roland, and G. N. Greaves, “An interpretation of quasielastic neutron scattering and molecular dynamics simulation results on the glass transition.,” *Journal of Non-Crystalline Solids*, vol. 182, pp. 172-179, 1995.
[44] V. A. Mashkov, W. R. Austin, L. Zhang, and R. G. Leisure, “Fundamental role of creation and activation in radiation-induced defect production in high-purity amorphous SIO2,” *Physical Review Letters*, vol. 76, pp. 2926-2929, 1996.
[45] C. Chabrerie, “De l'utilisation des recuits isothermes et isochrones pour la caractérisation de structures MOS irradiées.,” : Paris 7, 1997.